Journal of Nonlinear Modeling and Analysis
Volume 7, Number 5, October 2025, 1575–1610
https://journal.global-sci.org/jnma
DOI:10.12150/jnma.2025.1575

A Caputo-Based Fractional Order Modelling of COVID-19 in Nigeria

Bolarinwa Bolaji[1,3], Benjamin Idoko Omede[1,3], Godwin Onuche Acheneje[1,3], William Atokolo[1,†] and Udoka Benedict Odionyenma[2]

Abstract Our focus in this work is the proposition of a fractional order model based on Caputo fractional derivatives for the understanding of how coronavirus disease is transmitted in a community, using Nigeria as a case study. By using Laplace transform, we show that the state variables of the model are non-negative at all times and show the existence and uniqueness of solutions for the model. Thorough analysis of the model shows that the model is Ulam-Hyers-Rassias stable and that its disease-free equilibrium is locally and globally asymptotically stable whenever the reproduction number of the disease is less than unity. By gathering real-life data about the disease in Nigeria from accredited authority, Nigerian Centre for Disease Control (NCDC), we estimate parameters driving the spread of the disease by fitting this data to our model. By adopting these parameter estimates, using MATLAB, we per-form the numerical simulation of the model with a view to validating results from qualitative analysis of the model. Numerical results show that plots for the model at different fractional orders have major determining influence on various compartments of the model as it varies. Various distinct results were observed for each of the compartments in different fractional orders, highlight-ing the importance of consideration of the fractional order in modelling the highly contagious COVID-19 disease. This work highlights the advantage of fractional order model over the classical integer order model in the sense that the solution obtained for the fractional order model possesses a higher degree of freedom that enables variation of the system so as to obtain as many prefer-able responses of the different classes as desired since variation of fractional order ξ can be done at any preferable fractional rate 0.7, 0.4, 0.2 etc.

Keywords Fractional order, Caputo derivatives, Laplace transform

MSC(2010) 26A33, 34A08, 34D20, 34D23, 92B05.

[†]the corresponding author.
Email address: bolarinwa.s.bolaji@gmail.com (Bolarinwa Bolaji), benjaminomede197@gmail.com (Benjamin Idoko Omede),achenejegodwin@gmail.com(Godwin Onuche Acheneje), williamsatokolo@gmail.com(Williams Atokolo) oudoka@aust.edu.ng(Benedict Odionyenma)
[1]Department of Mathematical Sciences, Prince Abubakar Audu University, 272102 Anyigba, Nigeria
[2]Department of Mathematics, African University of Science and Technology, Galadima 900107, Nigeria
[3]Laboratory of Mathematical Epidemiology and Applied Sciences, Prince Abubakar Audu, 272102 Anyigba, Nigeria

1. Introduction

The origin of COVID-19 which is a deadly, highly contagious disease caused by Severe Acute Respiratory Syndrome coronavirus 2 (SARS-COV-2) is Wuhan city of China [1]. It has its mode of transmission from human to human through direct contact with infected persons and surfaces that are contaminated droplets from infected individuals [2]. It is revealed through clinical evidences that COVID-19 has its incubation period of 2 to 14 days [3–5,8], the period during which infected individuals with the disease start showing clinical symptoms of the highly communicable disease. The infected individuals with the disease during this period of incubation may or may not show symptoms of the disease; regrettably, they are capable of transmitting the disease to other individuals that they come in contact with. Coughing, breathing difficulties, and fever are the symptoms of the disease [9]. It is reported that as of November 6th, 2022, with 6.5 million reported deaths globally [4,10]. For now, the deadly disease do not have a clinically proven drug to combat its spread, though there are lots of control measures to combat the spread of the disease, such as regular usage of nose masks while in public, regular hand washing with soap or sanitizers and observance of social distances while in public space [5, 11, 12]. The good news is that there is availability of clinically proven vaccines to combat the spread of the disease, which include: the mRNA-1273 Moderna vaccine, BNT162b2 Pfizer-BioNtech vaccine and a highly efficacious vaccine against different variants of CPVID-19 developed in the United States, Johnson and Johnson vaccine [6,7].

As soon as the COVID-19 pandemic started ravaging the whole world, mathematical epidemiologists went to their studying table to complement the works of the healthcare providers and policy makers in health sectors to combat the spread of the deadly disease by developing several mathematical models including the ones in [10, 11, 13–18, 20–26]. In the work of Gumel et al. [16], a primer for COVID-19 was established. Their work was used to have an understanding of how the disease was transmitted in the early stage of the pandemic in the USA. Okunoghae and Omame [18], in the works on modelling of the transmission dynamics of disease in Nigeria, they incorporated three COVID-19 safety protocols: use of face masks while in public, regular hand washing with soap and hand sanitizers and maintenance of social distance while in public into their model and obtain thresholds for the percentage of the usage of these safety protocols to ensure that the affliction arising from the pandemic is mitigated in the community. Sowole et al. [25] in their work explored and incorporated a linear regression method into the model they proposed and used this to make forecast about the early stage of the disease. Omame et al. [20] in their work proposed a model formulated using fractional calculus with fractional order to study the spread of the co-infection of COVID-19 and Hepatitis B virus, using real-life data from Wuhan city of China. They illustrated that transmission rate for each of the two diseases can have a great impact on the dynamics of the co-infection of the two diseases and to have adequate and effective control of the interaction between the two disease in the population under reference, there is need for concerted efforts to be exerted towards the prevention of infection of either or both diseases.

Due to limitation of classical integer order derivatives, its inability to capture the memory effect, modelling of communicable diseases using fractional order derivatives incorporating fractional differential operators with its merit being that it can capture memory effects which is the major motivation for the development of such

fractional differential operators, is the current vogue and it is of considerable interest to mathematical epidemiology. In literature, many researchers have made significant contributions to the concept of fractional calculus, giving definitions of fractional-order operators that are applicable in modelling of epidemiological model in terms of system of non-linear fractional order differential equation, these include Reimann-Liouville [28], Weyl [30], Davidson and Essex [34], Coimbra [21], Jumarie [32, 33], Riesz [27], Hadamard [29] and Atagana [27]. Each of these researchers gave definitions to derivative of functions in fractional order in their unique ways, though some of their works are with limitations (see the work of Omame et al. [20]). To step over the drawbacks of the limitations inherent in the works of researchers in Ref. [**?**, 15–19] mentioned above, Atangana and Baleanu (AB) [27] and Caputo and Fabrizio (CF) [35] in their works provided us with a more improved definitions of fractional-order operators that will help in obtaining fractional order epidemiological model. Their works are based on the generalized Mittag-Leffler function and exponential kernel respectively [20]. Also, El-Mesady et al. [53] presented a fractional order model for TB transmission focusing on individuals with underlying ailments. Their study highlights vaccination and awareness as key control measures which offer useful insights for TB intervention strategies. Peter et al. [54] developed a measles model separating first- and second-dose vaccinations and used fractional calculus for analysis. The study highlights that increasing vaccination coverage effectively reduces measles spread and disease burden. Addai et al. [55] developed a fractal-fractional age-structured smoking model with government intervention, proving existence, uniqueness, and stability of solutions. Their study showed that changes in fractal-fractional orders and interventions significantly affect smoking dynamics across age groups. Yadav et al. [56] developed a fractional order diabetes mellitus model using the ABC derivative, proving existence and uniqueness of solutions via Picard's theorem. Numerical simulations revealed that decreasing the fractional order increases diabetes prevalence. Their study offers valuable insights into diabetes dynamics and potential extensions to coexisting diseases like tuberculosis. Abioye et al. [57] modelled malaria and COVID-19 co-infection with fractional derivatives, proving solution uniqueness and stability. Simulations showed that preventive measures can reduce and potentially eliminate the co-infection of these diseases. Peter et al. [58] developed a fractional ABC derivative model for meningitis, analyzed the stability and backward bifurcation, and examined vaccination and treatment effects on disease control. Peter et al. [59] developed a fractional monkeypox model, fitted it to Nigerian data, proved stability for the basic reproduction number being less than unity and used simulations to suggest control strategies. Abioye et al. [59] developed a fractional-order mathematical model to analyze COVID-19 transmission dynamics in Nigeria using the Atangana-Baleanu fractional derivative operator. They investigated the stability analysis of the disease-free and endemic equilibrium points, performed sensitivity analysis to identify key parameters affecting disease spread, and demonstrated that the fractional-order model provides better fitting to real COVID-19 data compared to classical integer-order models. Peter et al. [61] formulated a fractional-order mathematical model for pneumococcal pneumonia infection dynamics using the Caputo-Fabrizio fractional derivative operator. They analyzed the stability of equilibrium points, investigated the basic reproduction number, and demonstrated that the fractional-order model with Caputo-Fabrizio operator provides more realistic disease dynamics compared to classical integer-order models, offering better insights

into the transmission patterns of pneumococcal pneumonia. Ojo et al. [62] developed a fractional-order epidemiological model to study brucellosis transmission dynamics using the Caputo-Fabrizio fractional derivative operator. They performed a comprehensive mathematical analysis including existence and uniqueness of solutions, stability analysis of disease-free and endemic equilibria, and numerical simulations to demonstrate that the fractional-order approach captures the memory effects and hereditary properties inherent in brucellosis transmission better than conventional integer-order models. Preference is now being given to the adoption of any of these methods in modelling of fractional order epidemiological models; consequently, we are motivated to choose Caputo and Fabrizio in this our study.

Researchers in applied sciences and mathematical epidemiology are formulating and deploying Caputo based and Atagana Baleanu fractional order models governed by systems of non-linear differential equations to study the transmission dynamics of highly contagious diseases, in the works such as those in [43–47]. We are motivated by these works. This model improves upon existing models by utilizing Caputo fractional derivatives to account for memory effects, by incorporating parameter estimates derived from real data from Nigeria, and by allowing for fractional-order variation to explore diverse system dynamics. These enhancements contribute to improved accuracy, relevance, and flexibility in simulating and understanding the spread of COVID-19 within the Nigerian context.

The importance of this study stems from its focus on applying fractional-order calculus, particularly Caputo derivatives, to model the spread of COVID-19 in Nigeria. The use of fractional-order models offers significant advantages over classical integer-order models, especially in capturing memory effects and long-term dependencies typical of real epidemics. By fitting the model to actual data obtained from the Nigerian Centre for Disease Control (NCDC), the study enhances the practical relevance of the results, ensuring that the findings are data-driven and context-specific. Furthermore, this work demonstrates that the fractional order ξ plays a crucial role in shaping the system's behavior, thereby offering a flexible tool for exploring various transmission dynamics and control scenarios. This modeling approach serves as a powerful framework for understanding, predicting, and ultimately managing infectious diseases like COVID-19 in real-world settings, particularly in resource-constrained environments. Fractional differential operators, particularly those in the Caputo sense, allow for the incorporation of memory effects into the system, thereby enhancing the realism of epidemiological models. This is essential for diseases like COVID-19, where the disease progression and transmission dynamics are influenced not only by the current state but also by the historical interactions and delays in response or treatment. The flexibility in varying the fractional order enables the capture of a wider spectrum of dynamic behaviors, making fractional-order models more adaptable and effective than their classical counterparts. The results from this study stand out in several key aspects compared with existing models of COVID-19. First, the model demonstrates that changes in the fractional order ξ lead to significantly different disease progression profiles across compartments, emphasizing the sensitivity of the system to memory effects inherent in fractional-order systems. This dynamic behavior is largely absent in traditional integer-order models. Second, the proof of Ulam-Hyers-Rassias stability adds mathematical depth, ensuring the robustness of the model against perturbations—a feature rarely addressed in similar studies. Furthermore, the use of the Laplace transform to establish non-negativity and uniqueness of solutions

enhances the mathematical validity of the model. By incorporating real data from the Nigerian Centre for Disease Control (NCDC) for parameter estimation, the study bridges theoretical modeling with practical relevance. Together, these results highlight the advantages and innovations of adopting a fractional-order modeling approach in analyzing and managing the spread of infectious diseases like COVID-19. By incorporating memory-dependent terms, fractional-order models like the one proposed in this work offer more accurate reflections of the temporal nature of infectious disease transmission and control. Unlike classical integer-order derivatives that describe instantaneous rates of change based only on the present state, the Caputo fractional derivative incorporates the historical states of the system via a singular kernel. This enables the model to capture memory effects inherent in the spread and control of infectious diseases such as COVID-19, allowing a more accurate reflection of real-life epidemic dynamics.

We structure the rest of the article as follows: in Section 2, we presented the preliminaries and how the fractional order model is formulated. In Section 3, we adopt Laplace transform to show that the state variables for the model are positive at all times, local and global stability of the model. In Section 4, we did the data fitting to model and we presented the numerical simulations of the fractional order model, while in Section 5 we present the summary, findings, recommendations and the conclusion for this work.

2. Preliminaries and how the fractional order model was formulated

Here in this section, we look at the preliminary information about what Caputo fractional order derivative is, giving necessary definitions associated with the concept.

Definition 2.1. We can define Caputo fractional order derivative of a function f (t) on the interval $[0, T]$ as:

$$\left[D_t^{\xi} f(t)\right] = J_t^{n-\xi} D^n f(t) = \frac{1}{\Gamma(n-\xi)} \int_0^t (t-\zeta)^{n-\xi-1} f^{(n)}(\zeta) d\zeta, \tag{2.1}$$

where n is an integer given by $n-1 < \xi \leq n$. Whenever $0 < \xi \leq 1$, from the derivative above, where $\varsigma > 0$, the Caputo derivative becomes:

$$\left[D_0^{\xi} f(t)\right] = \frac{1}{\Gamma(1-\xi)} \int_0^t (t-\zeta)^{-\xi} f'(\zeta) d\zeta.$$

Definition 2.2. We define the fractional integral of order $\varsigma > 0$ of a function $f \in C^1(0, T)$ as:

$$J_t^{\xi} f(t) = \frac{1}{\Gamma(\xi)} \int_0^t (t-\zeta)^{\xi-1} f(\zeta) d\zeta,\ t > 0,$$

given that the integral exists in $\Re^+$. For convenience, suppose$f(t) = K$, where K is a constant. Then:

$$J_t^{\xi} f(t) = \frac{1}{\Gamma(\xi)} \int_0^t (t-\zeta)^{\varsigma-1}(K)d\zeta = K\frac{t^{\xi}}{\Gamma(\xi+1)}. \tag{2.2}$$

Definition 2.3. The Laplace transform of Caputo fractional derivative is defines as:

$$L\left\{D_0^{\xi} f(t)\right\} = s^{\xi}\bar{f}(s) - s^{\xi-1}f(0), \tag{2.3}$$

$0 < \xi \leq 1$, where L is the Laplace transform operator.

Lemma 2.1. *Suppose that $\xi \in \Re_+^8$ is such that $\vartheta_1(t)$and $\vartheta_2(t)$represent positive functions and $\vartheta_3(t)$ represents an increasing and positive function for $0 \leq t \leq T$, with $T > 0$ and $\vartheta_3(t) < N$ for N being a constant. Given that:*

$$\vartheta_1(t) \leq \theta\vartheta) + \vartheta_3(t) \int_0^t (t-\zeta)^{\xi-1}\theta_1(\zeta)d\zeta,$$

then

$$\vartheta_1(t) \leq \vartheta_2(t)E_{\xi}\left(\vartheta_3(t)\frac{\pi}{\Gamma(\xi-1)\sin(\pi\xi)}T^{\xi}\right).$$

In the work of Omede et al. [10], the authors proposed a mathematical model carefully designed to understand of the transmission dynamics of COVID-19 where demographic parameters are not incorporated.

The proposed model is as given below:

$$\begin{aligned}
\frac{dS}{dt} &= -\frac{\beta_c(1-\rho_1)(1-\rho_2)(1-\tau_1)(c_1A+I+c_2M)S}{N} - vS + \mu Q,\\
\frac{dE}{dt} &= \frac{\beta_c(1-\rho_1)(1-\rho_2)(1-\tau_1)(c_1A+I+c_2M)S}{N} - (\alpha+\sigma)E,\\
\frac{dQ}{dt} &= \alpha E - (\eta+\mu)Q,\\
\frac{dA}{dt} &= k\sigma E - (\omega+\varepsilon_A)A,\\
\frac{dI}{dt} &= (1-k)\sigma E - (q+\delta_I+\varepsilon_I)I,\\
\frac{dM}{dt} &= (1-\tau_2\phi)qI - (\theta+\delta_M+\varepsilon_M)M,\\
\frac{dI_H}{dt} &= \eta Q + \omega A + \tau_2\phi qI + \theta M - (\gamma+\delta_H)I_H,\\
\frac{dR}{dt} &= \varepsilon_A A + \varepsilon_I I + \varepsilon_M M + \gamma I_H + vS,
\end{aligned} \tag{2.4}$$

where the total human population at time t, is denoted by $N(t)$ and divided into eight mutually exclusive compartments of: Susceptible humans $S(t)$, Exposed humans $E(t)$, Quarantined humans $Q(t)$, Undetected asymptomatic infectious humans $A(t)$, Undetected symptomatic infectious humans $I(t)$, Undetected symptomatic infectious humans under self-medication $M(t)$, Detected and Hospitalized

infectious humans (via testing) $I_H(t)$and Recovered humans $R(t)$. So we have:

$$N(t) = S(t) + E(t) + Q(t) + A(t) + I(t) + M(t) + I_H(t) + R(t).$$

The underlying assumptions supporting the formulation of the COVID-19 model in (2.4) are presented below:

1. COVID-19 transmission is primarily driven by contact with infectious individuals. Susceptible individuals contract the virus through effective contact with both symptomatic and asymptomatic infectious individuals. This is consistent with the established epidemiology of COVID-19, where asymptomatic and presymptomatic carriers contribute significantly to community transmission [48].
2. Asymptomatic and self-medicating individuals transmit the virus at a reduced rate.
   The model incorporates modification parameters c_1 and c_2 to represent reduced infectivity from the asymptomatic $A(t)$ and self-medicating $M(t)$ classes. Studies have shown that while these individuals can transmit SARS-CoV-2, their viral load and transmission likelihood are generally lower than those of symptomatic individuals receiving no intervention [49, 50].
3. Quarantine and early detection reduce disease progression and community spread.
   Exposed individuals are quarantined at rate α, and infectious individuals are detected through testing or monitoring at rates ω and q. Quarantine and detection are widely adopted public health measures that reduce secondary infections and allow timely clinical intervention [51].
4. Non-pharmaceutical interventions (NPIs) effectively reduce the force of infection.
   The model accounts for population-level compliance with NPIs such as mask usage ρ_1, hand hygiene ρ_2, and social distancing τ_1. These interventions are proven to significantly reduce SARS-CoV-2 transmission, especially before widespread vaccine availability [52].

The susceptible individuals make contact with COVID-19 infected individuals at the rate β_c.They comply with wearing of face masks at the rate ρ_1, and they comply with to frequent washing of hands with soap and hand sanitizers at the rate ρ_2, while they comply with the maintenance of social distancing at the rate τ_1. Vaccinate rate for those vaccinated against the disease is v; exposed humans that are quarantined occur at rate α, the rate at which latently infected humans that are quarantined and do not develop symptoms that progress to susceptible class again is μ, while $c_1(c_2)$ is the modification parameter that accounts for a reduced transmission from A(M) class respectively. The rate of progression from exposed class to infectious class is given by σ The rate of death arising from the disease for those symptomatic infected individuals that are undetected, those infectious individuals that are detected, hospitalized and those individuals that are treating themselves is ε_A (ε_I)respectively. The rate at which disease-induced death occur for individuals that are symptomatically infectious but undetected, infectious individuals that are detected and receiving treatment in the hospital, individuals that are treating themselves is $\delta_I(\delta_H)$ respectively. Those individuals that are on

self-medication progressed to hospitals treatment at the rate θ, sensitization against self-medication occur at the rate ϕ, while the rate at which detection via testing occurs for infectious individuals that are asymptomatic but undetected is ω. The rate of transition for infectious individuals that are undetected symptomatic is q; the individuals that are quarantine progress to the class of detected infectious hospitalized at the rate η, the rate at which the fraction of those infectious individuals that are symptomatic adhere strictly to safety protocols associated with COVID-19 and avoid self-medication is τ_2 while those infectious individuals that are detected and hospitalized recovered at the rate γ.

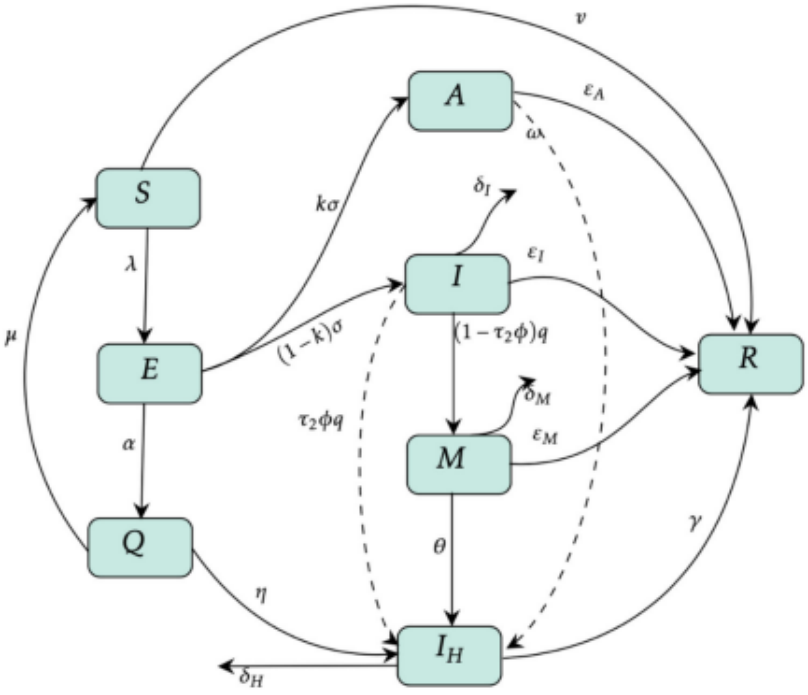

Figure 1. Schematic diagram of the COVID-19 model

The description of parameters of model (2.1) is as given in the table below.

Parameters	Description	Values	References
β_c	Effective contact rate.	0.4	Fitted
ρ_1	Rate at which individuals comply with wearing of face mask.	0.1	[5]
ρ_2	Rate at which individuals comply with washing of hands with soap and hand sanitizer	0.2	[20]
τ_1	Rate at which individuals comply with maintenance of social distancing.	0.2	[20]
v	Vaccination rate.	0.1582	[12]
α	Rate at which latently infected individuals are quarantined through contact tracing.	1/7	Estimated
μ	Rate at which latently infected asymptomatic individuals that are quarantined progress back to susceptible class.	0.025	Assumed
c_1	Modification parameter that accounts for a reduced transmission from A class.	0.5	[23]
c_2	Modification parameter that accounts for increased transmission from M class.	0.4341	Assumed
σ	Rate at which latently infected individuals progress to infected class	1/5	[21]
k	Part of new individuals that are infectious but not showing symptoms.	0.25	[23]
$\varepsilon_A(\varepsilon_I)$	Rate of disease-induced death for undetected asymptomatic, detected hospitalized, and self-medicated infectious individuals.	1/7 (1/7)	[34, 35]
ε_M	Rate at which individuals progress from self-medicated class to infected hospitalized class.	1/7	[34, 35]
δ_I	Disease-induced death rate for undetected symptomatic infectious individuals.	0.015	[33]
δ_H	Disease-induced death rate for hospitalized infectious individuals.	0.21	Assumed
δ_M	Disease-induced death rate for individuals on self-medication.	0.015	[33]
θ	Rate of progression from self-medication to hospitalized class.	0.164	Fitted
ϕ	Rate of sensitization on the danger of self-medication.	0.01	Assumed
ω	Detection rate for undetected asymptomatic infectious individuals.	2.2719×10^{-11}	Fitted
q	Transition rate for undetected symptomatic infectious individuals.	0.04	Fitted

Table 1. Description of parameters in the model (2.4).

η	Rate of progression of quarantined individuals to hospitalized detected infectious class.	0.514	Fitted
γ	Treatment-induced recovery rate for hospitalized detected infectious individuals.	1/15	[23, 32]
τ_2	Fraction of undetected symptomatic infectious individuals complying with safety protocols.	0.0135	[20]

Table 2. Description of parameters in the model (2.4).

On the adoption of definition 2.1, 2.2 and 2.3 above on model (2.4) so as to reformulate it as a system of fractional order ξ for $0 < \xi < 1$ differential equations, we obtained:

$$\begin{aligned}
D_t^{\xi} S(t) &= -\frac{\beta_c (1-\rho_1)(1-\rho_2)(1-\tau_1)(c_1 A + I + c_2 M) S}{N} - vS + \mu Q \cong Q(t, S(t)), \\
D_t^{\xi} E(t) &= -\frac{\beta_c (1-\rho_1)(1-\rho_2)(1-\tau_1)(c_1 A + I + c_2 M) S}{N} - (\alpha + \sigma) E \cong T(t, E(t)), \\
D_t^{\xi} Q(t) &= \alpha E - (\eta + \mu) Q \cong U(t, Q(t)), \\
D_t^{\xi} A(t) &= k\sigma E - (\omega + \varepsilon_A) A \cong V(t, A(t)), \\
D_t^{\xi} I(t) &= (1-k)\sigma E - (q + \delta_1 + \varepsilon_I) I \cong W(t, I(t)), \\
D_t^{\xi} M(t) &= (1-\tau_2\varphi) qI - (\theta + \delta_M + \varepsilon_M) M \cong X(t, M(t)), \\
D_t^{\xi} I_H(t) &= \eta Q + \omega A + \tau_2 \varphi q I + \theta M - (\gamma + \delta_H) I_H \cong Y(t, I_H(t)), \\
D_t^{\xi} R(t) &= \varepsilon_A A + \varepsilon_1 I + \varepsilon_M M + \gamma I_H - vS \cong Z(t, R(t)),
\end{aligned} \tag{2.5}$$

where

$$N(t) = S(t) + E(t) + Q(t) + A(t) + I(t) + M(t) + I_H(t) + R(t)$$

and $\xi \in (0, 1]$.

With initial conditions:
$S(0) \geq 0$, $E(0) \geq 0$, $Q(0) \geq 0$, $A(0) \geq 0$, $I(0) \geq 0$,
$M(0) \geq 0$, $I_H(0) \geq 0$ and $R(0) \geq 0$.

3. Basic properties analysis of the model (2.5)

It is pertinent to examine the basic properties of the proposed fractional order model (2.4), this is what we do in this section.

3.1. Positive invariance

Theorem 3.1. *Given that the solution of the fractional order model (2.5) is* $S(t)$, $E(t), Q(t), A(t), I(t), M(t), I_H, R(t)$, *then the set:*

$$\begin{aligned}
\Omega = \{&(S(t), E(t), Q(t), A(t), I(t), M(t), I_H, R(t)) \in \\
&\Re_+^8 : S(t) + E(t) + Q(t) + A(t) + I(t) + M(t) + I_H + R(t) \leq \frac{\pi}{\mu}\Big\}.
\end{aligned} \tag{3.1}$$

Consequently, this set of solution is positively invariant.

Proof. In addition, all the equations of the proposed model (2.5) give:

$$\begin{aligned} &D_t^{\varsigma} N \\ =&D_t^{\varsigma} S(t) + D_t^{\varsigma} E(t) + D_t^{\varsigma} Q(t) + D_t^{\varsigma} A(t) + D_t^{\varsigma} I(t) + D_t^{\varsigma} M(t) + D_t^{\varsigma} I_H + D_t^{\varsigma} R(t) \\ =&\pi - (S + E + Q + A + I + M + I_H + R)\,\mu - (\delta_I I + \delta_M M + \delta_H I_H) \\ \leq&\pi - \mu N. \end{aligned}$$

By applying Laplace transform to both sides of this, we obtain:

$$s^{\xi}\tilde{N}(s) - s^{\xi-1}N(0) \leq \frac{\pi}{s} - \mu\tilde{N}(s),$$

Simplifying this, we obtain:

$$\tilde{N}(s) \leq \frac{\pi}{s\left(s^{\xi}+\mu\right)} + N(0)\frac{s^{\xi-1}}{s^{\xi}+\mu}.$$

By resolving the fractions on the right hand side of this into its components, we have:

$$\tilde{N}(s) \leq \frac{\pi}{s}\left(\frac{1}{s}\right) - \left(\frac{\pi}{s} - N(0)\right)\sum_{i-0}^{\infty}\frac{(-\mu)^i}{s^{\xi i+1}}.$$

By taking the inverse Laplace transform of this we have:

$$N(t) \leq \frac{\pi}{s} - \left(\frac{\pi}{s} - N(0)\right)E_{\xi}\left(-\mu t^{\xi}\right),$$

as $t \to \infty$ and the inequality above becomes:

$$N\left(t\right) \leq \frac{\pi}{\mu}. \tag{3.2}$$

Showing that the equations in the fractional order co-infection model (2.5) are bounded, thus, the co-infection model is said to be mathematically well-posed and biologically meaningful. □

3.2. Positivity of solution to the equations in the co-infection model (2.5)

By logical inconsistency, suppose that we accept that the fourth condition of the model is not true in the spirit of the thoughts of Ugochukwu et al. [37].

Let $t_1 = \min\{t : S(t), E(t), Q(t), A(t), I(t), M(t), I_H, R(t)\}$. Given that $A(t_1) = 0$, it gives rise to $S(t) > 0, E(t) > 0, Q(t) > 0, A(t) > 0, I(t) > 0, M(t) > 0, I_H > 0 \text{and} R(t) > 0$ for all $[0, t_1]$. Given that the following expression holds:

$$\vartheta_1 = \min_{0\leq t\leq t_i}\left\{\frac{k\sigma E}{A} - (\omega + \varepsilon_A)\right\}.$$

This gives rise to

$$D_t^{\varsigma} A(t) - \vartheta_1 A(t) > 0. \tag{3.3}$$

The following equation is established since Λ_1 is a continuous function

$$D_t^{\varsigma} A(t) - \vartheta_1 A(t) = \Lambda_1(t).$$

By taking the Laplace transform of this we obtain:

$$s^{\xi}\bar{A}(s) - s^{\xi-1}A(0) - \vartheta_1\bar{A}(s) = -\bar{\Lambda}_1(t).$$

Arising from here we got:

$$\begin{aligned}\bar{A}(s) =& A(0)\frac{s^{\xi-1}}{s^{\xi}-\vartheta_1} - \frac{\Lambda_1(s)}{s^{\xi}-\vartheta_1} = \frac{A(0)}{s}\left(1-\frac{\vartheta_1}{s^{\xi}}\right)^{-1} - \frac{\Lambda_1(s)}{s^{\xi}}\left(1-\frac{\vartheta_1}{s^{\xi}}\right)^{-1}\\ =& A(0)\sum_{i=0}^{\infty}\frac{\vartheta_1^i}{s^{\xi i+1}} - \Lambda_1(s)\sum_{i=0}^{\infty}\frac{\vartheta_1^i}{s^{\xi i+1}}.\end{aligned}$$

By utilizing the Mittag Leffler function and by taking the inverse Laplace transform of this produced solution to (3.3) where, the following expression is obtained:

$$A(t) > A(0)\sum_{i=0}^{\infty}\frac{\left(\vartheta_1 t^{\xi}\right)^i}{\Gamma\xi i+1} = A(0)E_{\xi}\left(\vartheta_1 t^{\xi}\right).$$

Consequently, the solution to $A(t)$ positivity gives rise to:

$$A(t) > A(0)E_{\xi}\left(\vartheta_1 t^{\xi}\right) > 0.$$

This is a contradiction to $A(t_1) = 0$. Likewise, assuming that $I(t_1) = 0$ implies that $S(t) > 0, E(t) > 0, Q(t) > 0, A(t) > 0, M(t) > 0, I_H > 0 \text{and} R(t) > 0$ for all $[0, t_1]$. Given that the following expression holds:

$$\vartheta_2 = \min_{0\leq t\leq t_i}\left\{\frac{(1-k)\,\sigma E}{I} - (q+\delta_1+\varepsilon_1)\right\}.$$

This gives rise to

$$D_t^{\varsigma} I(t) - \vartheta_2 I(t) > 0. \tag{3.4}$$

The following equation is established since Λ_2 is a continuous function:

$$D_t^{\varsigma} I(t) - \vartheta_2 I(t) = -\Lambda_2(t).$$

By taking the Laplace transform of this we obtain:

$$s^{\xi}\tilde{I}(s) - s^{\xi-1}I(0) - \vartheta_1\tilde{I}(s) = -\bar{\Lambda}_2(t).$$

From here we obtain:

$$\begin{aligned}\tilde{I}(s) =& I(0)\frac{s^{\xi-1}}{s^{\xi}-\vartheta_2} - \frac{\Lambda_1(s)}{s^{\xi}-\vartheta_2} = \frac{I(0)}{s}\left(1-\frac{\vartheta_2}{s^{\varsigma}}\right)^{-1} - \frac{\Lambda_2(s)}{s^{\varsigma}}\left(1-\frac{\vartheta}{s^{\xi}}\right)^{-1}\\ =& I(0)\sum_{i=0}^{\infty}\frac{\vartheta_2^i}{s^{\xi i+1}} - \Lambda_2(s)\sum_{i=0}^{\infty}\frac{\vartheta_2^i}{s^{\xi i+1}}.\end{aligned}$$

By utilizing the Mittag-Leffler function and taking the inverse Laplace transform of this produced solution to (3.3) where, the following expression is obtained:

$$I(t) > I(0)\sum_{i=0}^{\infty}\frac{\left(\vartheta_2 t^{\xi}\right)^i}{\Gamma\left(\xi i+1\right)} = I(0)E_{\xi}\left(\vartheta_2 t^{\xi}\right).$$

Consequently, the solution to $I(t)$ positivity gives rise to:

$$I(t) > I(0)E_{\xi}\left(\vartheta_2 t^{\xi}\right) > 0,$$

which is a contradiction to $I(t_1) = 0$.

Likewise, by following the same approach as we did above, it can be shown that the positivity of solutions $S(t), E(t), Q(t), M(t), I_H$ and $R(t)$ is given respectively by:

$S(t) > S(0)E_{\xi}\left(\vartheta_3 t^{\xi}\right) > 0$, $E(t) > E(0)E_{\xi}\left(\vartheta_4 t^{\xi}\right) > 0$, $Q(t) > Q(0)E_{\xi}\left(\vartheta_5 t^{\xi}\right) > 0$,

$M(t) > M(0)E_{\xi}\left(\vartheta_6 t^{\xi}\right) > 0$, $I_H(t) > I_H(0)E_{\xi}\left(\vartheta_7 t^{\xi}\right) > 0$, $R(t) > R(0)E_{\xi}\left(\vartheta_8 t^{\xi}\right) > 0$.

3.3. Existence and uniqueness of solution to the equations of the co-infection model (2.5)

To establish the existence and uniqueness of a solution to the model, we adopt Schaefer's fixed point theorem, which requires that the system satisfy continuity and Lipschitz conditions, and that the associated solution operator be compact and map a closed, bounded, convex subset of a Banach space into itself. These conditions ensure that the model possesses at least one unique solution that is biologically feasible and mathematically stable. For our fractional order co-infection model (2.5), it becomes imperative to show the existence and uniqueness of its solution. By making use of the technique adopted by Ndolane [38] which involves using Banach fixed point theorem together with Schaefer's fixed point theorem we shall establish the existence of a solution to the proposed model and show the boundedness of the model. This method is characterized by applying the fractional integral to Caputo fractional order derivatives model (2.5) of order $\xi > 0$ together with its respective initial conditions so that the process leads to Volterra-integral equations that will serve as the basis for the solution to the proposed model (2.5). Suppose that Q, T, U, V, W, X, Y and Z are the right-hand sides of each of the model equations in (2.5). Then,

$$
\begin{aligned}
S(t)-S(0) &= \frac{1}{\Gamma(\xi)}\int_0^t (t-\varsigma)^{\xi-1} Q(t,S(t))\,d\varsigma,\\
E(t)-E(0) &= \frac{1}{\Gamma(\xi)}\int_0^t (t-\zeta)^{\xi-1} T(t,E(t))\,d\zeta,\\
Q(t)-Q(0) &= \frac{1}{\Gamma(\xi)}\int_0^t (t-\zeta)^{\xi-1} U(t,Q(t))\,d\zeta,\\
A(t)-A(0) &= \frac{1}{\Gamma(\xi)}\int_0^t (t-\zeta)^{\xi-1} V(t,A(t))\,d\zeta,\\
I(t)-I(0) &= \frac{1}{\Gamma(\xi)}\int_0^t (t-\zeta)^{\xi-1} W(t,I(t))\,d\zeta,\\
M(t)-M(0) &= \frac{1}{\Gamma(\xi)}\int_0^t (t-\zeta)^{\xi-1} X(t,M(t))\,d\zeta,\\
I_H(t)-I_H(0) &= \frac{1}{\Gamma(\xi)}\int_0^t (t-\zeta)^{\xi-1} Y(t,I_H(t))\,d\zeta,\\
R(t)-R(0) &= \frac{1}{\Gamma(\xi)}\int_0^t (t-\zeta)^{\xi-1} Z(t,S(t)d\zeta)\,.
\end{aligned}
\tag{3.5}
$$

Functions $(Q,T,U,V,W,X,Y,Z):[0,T]\times B\to B$ are assumed to be continuous and $(B,\|.\|)$ is a Banach space and provided that all the continuous functions that are defined in $[0,T]\to B$ shaped with Chebyshev norm have their Banach space being$A^1([0,T])$.

Our task is to show that the continuous functions $Q,T,U,V,W,X,Y,$ and Z satisfy the Lipchitz condition if:

$$
\begin{aligned}
&\sup_{0<t\le T}\left\|\tfrac{S(t)}{N(t)}\right\|\le\Omega_1,\\
&\sup_{0<t\le T}\left\|\tfrac{E(t)}{N(t)}\right\|\le\Omega_2,\ \sup_{0<t\le T}\left\|\tfrac{Q(t)}{N(t)}\right\|\le\Omega_3,\\
&\sup_{0<t\le T}\left\|\tfrac{A(t)}{N(t)}\right\|\le\Omega_4,\\
&\sup_{0<t\le T}\left\|\tfrac{I(t)}{N(t)}\right\|\le\Omega_5,\ \sup_{0<t\le T}\left\|\tfrac{M(t)}{N(t)}\right\|\le\Omega_6,\\
&\sup_{0<t\le T}\left\|\tfrac{I_H(t)}{N(t)}\right\|\le\Omega_7,\ \sup_{0<t\le T}\left\|\tfrac{R(t)}{N(t)}\right\|\le\Omega_8.
\end{aligned}
$$

Hence,

$$
\begin{aligned}
&\|Q(S_1)-Q(S_2)\|\\
&=\left\|\left[-\frac{\beta_c(1-\rho_1)(1-\rho_2)(1-\tau_1)(c_1A+I+c_2M)S}{N}-vS\right]S_1+\mu Q\right.\\
&\quad\left.-\left[-\frac{\beta_c(1-\rho_1)(1-\rho_2)(1-\tau_1)(c_1A+I+c_2M)S}{N}-vS\right]S_2+\mu Q\right\|\\
&=\left\|-\frac{\beta_c c_1 A}{N}(S_1-S_2)-\frac{\beta_c I}{N}(S_1-S_2)-\frac{\beta_c c_2 M}{N}(S_1-S_2)\right.\\
&\quad\left.-\frac{(1-\rho_1)(1-\rho_2)(1-\tau_1)}{N}(S_1-S_2)-v(S_1-S_2)\right\|
\end{aligned}
$$

$$
\begin{aligned}
&\leq \beta_c \sup_{0<t\leq T}\left\|\frac{c_1 A(t)}{N(t)}\right\|\|S_1-S_2\|+\beta_c \sup_{0<t\leq T}\left\|\frac{I(t)}{N(t)}\right\|\|S_1-S_2\| \\
&\quad+\beta_c \sup_{0<t\leq T}\left\|\frac{c_2 M(t)}{N(t)}\right\|\|S_1-S_2\|+\frac{(1-\rho_1)(1-\rho_2)(1-\tau_1)}{N}\|S_1-S_2\|+v\|S_1-S_2\| \\
&\leq J_Q\|S_1-S_2\|, \qquad (3.6)
\end{aligned}
$$

where $J_Q=\left(\beta_c\Omega_4+\beta_c\Omega_5+\beta_c\Omega_6+\frac{(1-\rho_1)(1-\rho_2)(1-\tau_1)}{N}+v\right)>0$.

Secondly, we have:

$$
\begin{aligned}
&\|T(S_1)-T(S_2)\| \\
&=\left\|\left[-\frac{\beta_c(1-\rho_1)(1-\rho_2)(1-\tau_1)(c_1A+I+c_2M)S_1}{N}-(\alpha+\sigma)E\right]\right. \\
&\quad\left.-\left[-\frac{\beta_c(1-\rho_1)(1-\rho_2)(1-\tau_1)(c_1A+I+c_2M)S_2}{N}-(\alpha+\sigma)E\right]\right| \\
&=\left\|-\frac{\beta_c c_1 A}{N}(S_1-S_2)-\frac{\beta_c I}{N}(S_1-S_2)-\frac{\beta_c c_2 M}{N}(S_1-S_2)\right. \\
&\quad\left.-\frac{(1-\rho_1)(1-\rho_2)(1-\tau_1)}{N}(S_1-S_2)\right\| \\
&\leq \beta_c \sup_{0<t\leq T}\left\|\frac{c_1 A(t)}{N(t)}\right\|\|S_1-S_2\|+\beta_c \sup_{0<t\leq T}\left\|\frac{I(t)}{N(t)}\right\|\|S_1-S_2\| \\
&\quad+\beta_c \sup_{0<t\leq T}\left\|\frac{c_2 M(t)}{N(t)}\right\|\|S_1-S_2\|+\frac{(1-\rho_1)(1-\rho_2)(1-\tau_1)}{N}\|S_1-S_2\| \\
&\leq J_T\|S_1-S_2\|, \qquad (3.7)
\end{aligned}
$$

where $J_T=\left(\beta_c\Omega_4+\beta_c\Omega_5+\beta_c\Omega_6+\frac{(1-\rho_1)(1-\rho_2)(1-\tau_1)}{N}\right)>0$.

Likewise, other functions U, V, W, X, Y and Z can be shown to satisfy Lipchitz condition in the same way.

Theorem 3.2. *Suppose* $(J_Q, J_T, J_U, J_V, J_W, J_X, J_Y, J_Z)\frac{\Gamma(1-\xi)\sin(\xi\pi)T^{\xi}}{\xi\pi}<1$. *This implies that the newly proposed model (2.5) has a unique solution on* $[0,T]$ *given that* $(Q,T,U,V,W,X,Y,Z):[0,T]\times B\to B$ *are continuous and satisfy Lipchitz Criteria.*

Proof. Let mapping τ: $A^1([0,T],B)\to A^1([0,T],B)$, given that τ is defined in $(Q,T,U,V,W,X,Y,Z):[0,T]\times B\to B$. By using (3.5)-(3.7) and for all $(S_1-S_2)\in A^1([0,T],B)$ and $0\leq t\leq T$, we obtain:

$$
\begin{aligned}
\|\tau(S_1(t)-\tau S_2(t))\| &= \left\|S(0)+\frac{1}{\Gamma(\xi)}\int_0^T(t-\zeta)^{\xi-1}F(t,S_1(t))\,d\zeta\right. \\
&\quad\left.-\left(S_2(0)+\frac{1}{\Gamma(\xi)}\int_0^T(t-\zeta)^{\xi-1}F(t,S(t))\,d\zeta\right)\right\| \\
&\leq \frac{1}{\Gamma(\xi)}\int_0^T(t-\zeta)^{\xi-1}\|F(t,S_1(t))-F(t,S_2(t))\|d\zeta \\
&\leq \frac{J_Q}{\Gamma(\xi)}\int_0^T(t-\zeta)^{\xi-1}\|S_1(t)-S_2(t)\|d\zeta
\end{aligned}
$$

$$\Rightarrow \|\tau\left(S_1(t)-\tau S_2(t)\right)\| \leq J_Q\left(\frac{T^{\xi}}{\Gamma\left(\xi+1\right)}\right)\|S_1(t)-S_2(t)\|_{A^1}.$$

The same process yields:

$$\Rightarrow \|\tau\left(S_1(t)-\tau S_1(t)\right)\| \leq J_T\left(\frac{T^{\xi}}{\Gamma\left(\xi+1\right)}\right)\|S_1(t)-S_2(t)\|_{A^1}. \tag{3.8}$$

Clearly,$(J_Q, J_T, J_U, J_V, J_W, J_X, J_Y, J_Z)\,\frac{\Gamma(1-\xi)\sin(\xi\pi)T^{\xi}}{\xi\pi} < 1$. The application of Banach contraction mapping reveals that on the interval $0 \leq t \leq T$, the operator τ has a distinct fixed point since because it is a contraction mapping.

□

This theorem guarantees the existence and uniqueness of a solution to the fractional-order epidemiological model proposed in the paper. From a biological perspective, this result confirms that the model behaves well-posedly; that is, for a given set of initial conditions and parameter values, the disease dynamics evolve in a predictable and consistent manner over time without ambiguity. In epidemiological modeling, such mathematical rigor is crucial. It ensures that the projected trajectories of infection, recovery, and other compartments are not artifacts of mathematical inconsistency but reflect the true underlying dynamics of disease spread. This reliability is essential when using the model for forecasting outbreaks, assessing intervention strategies, or conducting sensitivity analysis. Moreover, the involvement of the fractional operator and Mittag-Leffler-type kernel through the condition $\frac{\Gamma(1-\xi)\sin(\xi\pi)T^{\xi}}{\xi\pi}$implies that the model incorporates memory effects—a biologically realistic feature in infectious disease transmission, where the current state depends not only on the present but also on the past history of the system. The Lipschitz condition and continuity of the operators reflect biological stability in the response of the disease model to changes in state variables over time. This ensures that small changes in initial infection levels or control interventions do not cause unpredictable or explosive changes in model output.

Next we investigate the existence of solutions to the proposed model (2.5) by using Schaefer's fixed point theorem.

Theorem 3.3. *Let* $(Q,T,U,V,W,X,Y,Z) : [0,T]\times B \to B$ *be continuous and Suppose that there exist constants* $(J_{Q1}, J_{T1}, J_{U1}, J_{V1}, J_{W1}, J_{X1}, J_{Y1}, J_{Z1}) > 0$ *such that:*

$\|F\left(t,S\right)\| \leq J_{Q1}\left(c+\|S\|\right)$,

$\|F\left(t,E\right)\| \leq J_{T1}\left(c+\|E\|\right)$, $\|F\left(t,Q\right)\| \leq J_{U1}\left(c+\|Q\|\right)$,

$\|F\left(t,A\right)\| \leq J_{V1}\left(c+\|A\|\right)$, $\|F\left(t,I\right)\| \leq J_{W1}\left(c+\|I\|\right)$,

$\|F\left(t,M\right)\| \leq J_{X1}\left(c+\|M\|\right)$,

$\|F\left(t,I_H\right)\| \leq J_{Y1}\left(c+\|I_H\|\right)$*and* $\|F\left(t,R\right)\| \leq J_{Z1}\left(c+\|R\|\right)$, *with arbitrary number* $0 < c \leq 1$. *Then there is at least one solution for our proposed model (2.4).*

Proof. From (3.8), the operator τ is continuous. Suppose that $\left\{S^{i+1}\right\}_{\infty}$,$\left\{E^{i+1}\right\}_{\infty}$, $\left\{Q^{i+1}\right\}_{\infty}$,$\left\{A^{i+1}\right\}_{\infty}$, $\left\{I^{i+1}\right\}_{\infty}$, $\left\{M^{i+1}\right\}_{\infty}$ $\left\{I_H^{i+1}\right\}_{\infty}$, and $\left\{R^{i+1}\right\}_{\infty}$ are sequences for

$S^{i+1} \to S^i$,$E^{i+1} \to E^i$, $Q^{i+1} \to Q^i$, $A^{i+1} \to A^i$, $I^{i+1} \to I^i$, $M^{i+1} \to M^i$,$I_H^{i+1} \to I_H^i$ and $R^{i+1} \to R^i$ in $A^1\left([0,T],B\right)$. Given that $0 \le t \le T$, we have:

$$\begin{aligned}
&\left\|\tau S^{i+1}(t) - \tau S^i(t)\right\| \\
=&\frac{1}{\Gamma(\xi)}\left\|\int_0^t (t-\zeta)^{\xi-1} F\left(t, S^{i+1}(t)\right) d\zeta - \int_0^t (t-\zeta)^{\xi-1} F\left(t, S^i(t)\right) d\zeta\right\| \\
\le&\frac{1}{\Gamma(\xi)}\int_0^t (t-\zeta)^{\xi-1}\left\|F\left(t, S^{i+1}(t)\right) - F\left(t, S^i(t)\right)\right\| d\zeta \\
\le&\frac{J_{Q1}T^{\xi}}{\Gamma(\xi+1)}\left\|S^{i+1}(t) - S^i(t)\right\| \\
\le&J_{Q1}\left(\frac{T^{\xi}}{\Gamma(\xi+1)}\right)\left\|S^{i+1}(t) - S^i(t)\right\|_{A^1},
\end{aligned} \tag{3.9}$$

with $\left\|S^{i+1}(t) - S^i(t)\right\|_A \to 0$ as $n \to \infty$. By following the same procedure, we obtain:

$$\begin{aligned}
\left\|\tau E^{i+1}(t) \to \tau E^i(t)\right\| &\le J_{T1}\left(\tfrac{T^{\xi}}{\Gamma(\xi+1)}\right)\left\|E^{i+1}(t) - E^i(t)\right\|_{A^1}, \\
\left\|\phi Q^{i+1}(t) \to \phi Q^i(t)\right\| &\le J_{U1}\left(\tfrac{T^{\xi}}{\Gamma(\xi+1)}\right)\left\|Q^{i+1}(t) - Q^i(t)\right\|_{A^1}, \\
\left\|\phi A^{i+1}(t) \to \phi A^i(t)\right\| &\le J_{V1}\left(\tfrac{T^{\xi}}{\Gamma(\xi+1)}\right)\left\|A^{i+1}(t) - A^i(t)\right\|_{A^1} \\
\left\|\phi I^{i+1}(t) \to \phi I^i(t)\right\| &\le J_{W1}\left(\tfrac{T^{\xi}}{\Gamma(\xi+1)}\right)\left\|I^{i+1}(t) - I^i(t)\right\|_{A^1}, \\
\left\|\phi M^{i+1}(t) \to \phi M^i(t)\right\| &\le J_{X1}\left(\tfrac{T^{\xi}}{\Gamma(\xi+1)}\right)\left\|M^{i+1}(t) - M^i(t)\right\|_{A^1}, \\
\left\|\phi I_N^{i+1}(t) \to \phi I_H^i(t)\right\| &\le J_{Y1}\left(\tfrac{T^{\xi}}{\Gamma(\xi+1)}\right)\left\|I_H^{i+1}(t) - I_H^i(t)\right\|_{A^1}
\end{aligned}$$

and

$$\left\|\phi R^{i+1}(t) \to \phi R^i(t)\right\| \le J_{Z1}\left(\tfrac{T^{\xi}}{\Gamma(\xi+1)}\right)\left\|R^{i+1}(t) - R^i(t)\right\|_{A^1},$$

where

$$\begin{gathered}
\left\|E^{i+1}(t) - E^i(t)\right\|_{A^1} \to 0,\ \left\|Q^{i+1}(t) - Q^i(t)\right\|_{A^1} \to 0, \\
\left\|A^{i+1}(t) - A^i(t)\right\|_{A^1} \to 0,\ \left\|I^{i+1}(t) - I^i(t)\right\|_{A^1} \to 0, \\
\left\|I^{i+1}(t) - I^i(t)\right\|_{A^1} \to 0, \left\|M^{i+1}(t) - M^i(t)\right\|_{A^1} \to 0, \\
\left\|I_H^{i+1}(t) - I_H^i(t)\right\|_{A^1} \to 0, \text{ and } \left\|R^{i+1}(t) - R^i(t)\right\|_{A^1} \to 0,
\end{gathered}$$

as $n \to \infty$. Therefore, the operator τ is continuous.

We then wish to show that operator τ is bounded on the set $A^1\left([0,T],B\right)$.

For each $S \in A_S$, $E \in A_E$,

$$\begin{gathered}
Q \in A_Q,\ A \in A_A,\ I \in A_I,\ M \in A_M, \\
I_H \in A_{I_H}, R \in A_R,
\end{gathered}$$

and for $d > 0$, there corresponds a value $e > 0$ where

$$\begin{gathered}
\|\tau S\| \le e,\ \|\tau E\| \le e, \quad \|\tau Q\| \le e, \quad \|\tau A\| \le e, \\
\|\tau I\| \le e, \quad \|\tau M\| \le e, \quad \|\tau I_H\| \le e, \quad \|\tau R\| \le e,
\end{gathered}$$

and the subset of Banach space of all continuous function on the interval $0 \le t \le T$ is defined as follows:

$$A_S = \left\{S \in A^1\left([0,T],B\right) : \|S\| \leq d\right\},$$
$$A_E = \left\{S \in A^1\left([0,T],B\right) : \|E\| \leq d\right\},$$
$$A_Q = \left\{S \in A^1\left([0,T],B\right) : \|Q\| \leq d\right\},\ A_A = \left\{S \in A^1\left([0,T],B\right) : \|A\| \leq d\right\},$$
$$A_I = \left\{S \in A^1\left([0,T],B\right) : \|I\| \leq d\right\},\ A_M = \left\{S \in A^1\left([0,T],B\right) : \|M\| \leq d\right\},$$
$$A_{I_H} = \left\{S \in A^1\left([0,T],B\right) : \|I_H\| \leq d\right\},\ A_R = \left\{S \in A^1\left([0,T],B\right) : \|R\| \leq d\right\}.$$

For any $0 \leq t \leq T$,

$$\begin{aligned}
\|\tau S\| &\leq \|S(0)\| + \frac{1}{\Gamma(\xi)} \int_0^t (t-\zeta)^{\xi-1} \|F(t,S(t))\| \, d(\zeta) \\
&\leq \|S(0)\| + \frac{\|F(t,S(t))\|}{\Gamma(\xi)} \int_0^t (t-\zeta)^{\xi-1} d(\zeta) \\
&\leq \|S(0)\| + J_{Q1}(c + \|S\|) \left(\frac{T^\xi}{\Gamma(\xi+1)}\right), \\
\|\tau S\| &\leq \|S(0)\| + J_{Q1}(c+d) \left(\frac{T^\xi}{\Gamma(\xi+1)}\right).
\end{aligned}$$

Similarly, we obtain:

$$\begin{aligned}
\|\tau E_c\| &\leq \|E(0)\| + J_{T1}(c+d)\left(\tfrac{T^\xi}{\Gamma(\xi+1)}\right), \\
\|\tau Q\| &\leq \|Q(0)\| + J_{U1}(c+d)\left(\tfrac{T^\xi}{\Gamma(\xi+1)}\right), \\
\|\tau A\| &\leq \|A(0)\| + J_{V1}(c+d)\left(\tfrac{T^\xi}{\Gamma(\xi+1)}\right), \\
\|\tau I\| &\leq \|I(0)\| + J_{W1}(c+d)\left(\tfrac{T^\xi}{\Gamma(\xi+1)}\right), \\
\|\tau M\| &\leq \|M(0)\| + J_{X1}(c+d)\left(\tfrac{T^\xi}{\Gamma(\xi+1)}\right), \\
\|\tau I_H\| &\leq \|I_H(0)\| + J_{Y1}(c+d)\left(\tfrac{T^\xi}{\Gamma(\xi+1)}\right),
\end{aligned}$$

and

$$\|\tau R\| \leq \|R(0)\| + J_{Z1}(c+d)\left(\tfrac{T^\xi}{\Gamma(\xi+1)}\right).$$

Let Λ map bounded sets into equal continuous sets in $A^1([0,T],B)$.

Whenever $0 \leq t_1 \leq t_2 \leq T$, then $S \in A_S$, $E \in A_E$, $Q \in A_Q$, $A \in A_A$, $I \in A_I$, $M \in A_M$, $I_H \in A_{I_H}$,$R \in A_R$, where $t_1, t_2 \in [0,T]$. Then

$$\begin{aligned}
&\|\tau S(t_1) \to \tau S(t_2)\| \\
=&\frac{1}{\Gamma(\xi)} \left\| \int_0^{t_1} (t_1-\zeta)^{\xi-1} F(t,S(t)) - \int_0^{t_2} (t_2-\zeta)^{\varsigma-1} F(t,S(t)) \right\| d(\zeta) \\
\leq&\frac{1}{\Gamma(\xi)} \left\| \int_0^{t_1} \left[(t_1-\zeta)^{\xi-1} - (t_2-\zeta)^{\xi-1}\right] F(t,S(t)) d(\zeta) + \int_{t_1}^{t_2} (t_2-\zeta)^{\xi-1} F(t,S(t))\, d(\zeta) \right\| \\
\leq&\frac{J_{Q1}(c+d)}{\Gamma(\xi)} \left\| \int_0^{t_1} \left[(t_1-\zeta)^{\xi-1} - (t_2-\zeta)^{\xi-1}\right] d(\zeta) + \int_{t_1}^{t_2} (t_2-\zeta)^{\xi-1} d(\zeta) \right\| \\
\Rightarrow&\|\tau S(t_1) \to \tau S(t_2)\| \leq \frac{J_{Q1}(c+d)\, T^\xi}{\Gamma(\xi+1)} \left(t_1^\xi - t_2^\xi + 2(t_2-t_1)^\xi\right).
\end{aligned}$$

Adopting similar approach gives:

$$\begin{aligned}
\|\tau E(t_1) \to \tau E(t_2)\| &\leq \tfrac{J_{T1}(c+d)T^{\xi}}{\Gamma(\xi+1)}\left(t_1^{\xi} - t_2^{\xi} + 2(t_2-t_1)^{\xi}\right),\\
\|\tau Q(t_1) \to \tau Q(t_2)\| &\leq \tfrac{J_{U1}(c+d)T^{\xi}}{\Gamma(\xi+1)}\left(t_1^{\xi} - t_2^{\xi} + 2(t_2-t_1)^{\xi}\right),\\
\|\tau A(t_1) \to \tau A(t_2)\| &\leq \tfrac{J_{V1}(c+d)T^{\xi}}{\Gamma(\xi+1)}\left(t_1^{\xi} - t_2^{\xi} + 2(t_2-t_1)^{\xi}\right),\\
\|\tau I(t_1) \to \tau I(t_2)\| &\leq \tfrac{J_{W1}(c+d)T^{\xi}}{\Gamma(\xi+1)}\left(t_1^{\xi} - t_2^{\xi} + 2(t_2-t_1)^{\xi}\right),\\
\|\tau M(t_1) \to \tau M(t_2)\| &\leq \tfrac{J_{X1}(c+d)T^{\xi}}{\Gamma(\xi+1)}\left(t_1^{\xi} - t_2^{\xi} + 2(t_2-t_1)^{\xi}\right),\\
\|\tau I_H(t_1) \to \tau I_H(t_2)\| &\leq \tfrac{J_{Y1}(c+d)T^{\xi}}{\Gamma(\xi+1)}\left(t_1^{\xi} - t_2^{\xi} + 2(t_2-t_1)^{\xi}\right),\\
\|\tau R(t_1) \to \tau R(t_2)\| &\leq \tfrac{J_{Z1}(c+d)T^{\xi}}{\Gamma(\xi+1)}\left(t_1^{\xi} - t_2^{\xi} + 2(t_2-t_1)^{\xi}\right).
\end{aligned}$$

As $t_1 \to t_2$, by following Arzela-Ascoli theorem, each of the inequalities above tends to zero. It becomes imperative to wish to show that:

$$U(\tau) = (S(t), E(t), Q(t), A(t), I(t), M(t), I_H(t), R(t)) \in A^1([0,T], B),$$

$$\begin{aligned}
&A^1([0,T], B) : (S(t), E(t), Q(t), A(t), I(t), M(t), I_H(t), R(t))\\
=&\lambda(S(t), E(t), Q(t), A(t), I(t), M(t), I_H(t), R(t))
\end{aligned}$$

is bounded for some $\lambda \in (0,1)$.

Given that $(S(t), E(t), Q(t), A(t), I(t), M(t), I_H, R(t)) \in U(\tau)$, such that $(S(t), E(t), Q(t), A(t), I(t), M(t), I_H(t), R(t)) = \lambda\tau(S(t), E(t), Q(t), A(t), I(t), M(t), I_H, R(t))$, for each $t_2 \in [0,T]$ it follows that:

$$\begin{aligned}
\|S(t)\| \leq& S(0) + \frac{1}{\Gamma(\xi)}\int_0^T (t-\zeta)^{\xi-1}\|F(t, S(t))\|\, d(\zeta)\\
\leq& S(0) + \frac{J_{Q1}}{\Gamma(\xi)}\int_0^T (t-\zeta)^{\xi-1}(c + \|S(t)\|)\, d(\zeta)\\
\leq& S(0) + \frac{cJ_{Q1}}{\Gamma(\xi)}\int_0^T (t-\zeta)^{\xi-1} d(\zeta) + \frac{J_{Q1}}{\Gamma(\xi)}\int_0^T (t-\zeta)^{\xi-1}\|S(t)\|\, d(\zeta)\\
\leq& S(0) + \left(J_{Q1}\frac{T^{\xi}}{\Gamma(\xi)}\right) + \left(J_{Q1}\frac{T^{\xi}}{\Gamma(\xi)}\right)\int_0^T (t-\zeta)^{\xi-1}\|S(t)\|\, d(\zeta)\\
\Rightarrow \|S(t)\| \leq& \left(S(0) + \frac{J_{Q1}T^{\xi}}{\Gamma(\xi)} D_{\varsigma}\left(V_{G1}T^{\xi}\right)\right) < \infty. \qquad (3.10)
\end{aligned}$$

Similarly, we obtain the following by applying the same approach:

$$\begin{aligned}
\|E(t)\| &\leq \left(E(0) + \tfrac{J_{T1}T^{\xi}}{\Gamma(\xi)} D_{\xi}\left(J_{T1}T^{\xi}\right)\right) < \infty,\\
\|Q(t)\| &\leq \left(Q(0) + \tfrac{J_{U1}T^{\xi}}{\Gamma(\xi)} D_{\xi}\left(J_{V1}T^{\xi}\right)\right) < \infty,\\
\|A(t)\| &\leq \left(A(0) + \tfrac{J_{V1}T^{\xi}}{\Gamma(\xi)} D_{\xi}\left(J_{V1}T^{\xi}\right)\right) < \infty,\\
\|I(t)\| &\leq \left(I(0) + \tfrac{J_{W1}T^{\xi}}{\Gamma(\xi)} D_{\xi}\left(J_{W1}T^{\xi}\right)\right) < \infty,\\
\|M(t)\| &\leq \left(M(0) + \tfrac{J_{X1}T^{\xi}}{\Gamma(\xi)} D_{\xi}\left(J_{X1}T^{\xi}\right)\right) < \infty,\\
\|I_H(t)\| &\leq \left(I_H(0) + \tfrac{J_{Y1}T^{\xi}}{\Gamma(\xi)} D_{\xi}\left(J_{Y1}T^{\xi}\right)\right) < \infty,\\
\|R(t)\| &\leq \left(R(0) + \tfrac{J_{Z1}T^{\xi}}{\Gamma(\xi)} D_{\xi}\left(J_{Z1}T^{\xi}\right)\right) < \infty.
\end{aligned}$$

Having shown that $U(\tau)$ is bounded, then, by Schaefer's fixed point theorem, τ possesses a fixed point and consequently, it is the solution of the model.

□

Theorem 3.3 establishes the existence of at least one solution to the proposed COVID-19 model formulated in system (2.4). From an epidemiological perspective, this result ensures that the mathematical formulation of the model reliably captures the real-world disease dynamics over time. The existence of a solution guarantees that for every initial state of the population and parameter set, the model will generate a meaningful trajectory describing how the disease spreads, progresses, and recovers in the population. This is crucial for validating the model as a tool for understanding the behavior of the epidemic under various control strategies and interventions. It confirms that the model is not only mathematically sound but also dependable for simulating the outbreaks and guiding public health decisions.

3.4. Reproduction number of the COVID-19 model

The basic reproduction number, denoted by $\mathcal{R}_0$, represents the average number of secondary infections produced by a single infectious individual in a completely susceptible population. Biologically, it serves as a threshold indicator that determines whether an infectious disease can invade and persist within a population. When $\mathcal{R}_0 < 1$, each infected individual generates fewer than one new case on average, leading to disease elimination over time. Conversely, when $\mathcal{R}_0 > 1$, the infection can spread in the population, potentially leading to an outbreak or endemicity. In the context of COVID-19, $\mathcal{R}_0$ provides critical insights into the intensity of transmission and guides the implementation of control strategies such as vaccination, quarantine, public sensitization, and adherence to non-pharmaceutical interventions. Therefore, reducing $\mathcal{R}_0$ below unity is a fundamental goal in the design of public health interventions aimed at controlling and eventually eradicating the disease.

The disease free equilibrium of the COVID-19 model (2.4) is given by:

$$\begin{aligned}\varepsilon_0 &= (S^*(t), E^*(t), Q^*(t), A^*(t), I^*(t), M^*(t), I^*{}_H(t), R^*(t)) \\ &= \left(\frac{\pi}{\mu}, 0, 0, 0, 0, 0, 0, 0\right). \end{aligned} \tag{3.11}$$

By adopting the approach proposed by [33], the F and V matrices which correspond to the new infection terms and other transfer terms of the disease respectively as captured in the fractional order model (2.5) respectively are given by:

$$F = \begin{bmatrix} 0 & 0 & \beta T c_1 & \beta T & \beta T c_1 & 0 \\ 0 & 0 & 0 & 0 & 0 & 0 \\ 0 & 0 & 0 & 0 & 0 & 0 \\ 0 & 0 & 0 & 0 & 0 & 0 \\ 0 & 0 & 0 & 0 & 0 & 0 \\ 0 & 0 & 0 & 0 & 0 & 0 \end{bmatrix} \text{ and } V = \begin{bmatrix} P_1 & 0 & 0 & 0 & 0 & 0 \\ -\alpha & P_2 & 0 & 0 & 0 & 0 \\ -k\sigma & 0 & P_3 & 0 & 0 & 0 \\ -(1-k)\sigma & 0 & 0 & P_4 & 0 & 0 \\ 0 & 0 & 0 & -P_5 & P_6 & 0 \\ 0 & -\eta & -\omega & -\tau_2\varphi_2 & 0 & P_7 \end{bmatrix},$$

where $T = (1-\rho_1)(1-\rho_2)(1-\tau_1)$, $P_1 = (\alpha+\sigma)$, $P_2 = (\eta+\mu)$, $P_3 = (w+\varepsilon_A)$, $P_4 = (q+\delta_1+\varepsilon_1)$, $P_5 = (1-\tau_2\varphi)$,$P_6 = (\theta+\delta_M+\varepsilon_M)$, and $P_7 = (\gamma+\delta_H)$.

The reproduction number is given by $R_0 = \rho\left\{FV^{-1}\right\}$ where ρ is the largest absolute value of the Eigen value of $\left(FV^{-1}\right)$.

Consequently,

$$R_0 = -\frac{\beta(1-\rho_1)(1-\rho_2)(1-\tau_1)}{NX_2}\left[\frac{c_1 k\sigma}{P_1P_3} + \frac{(1-k)\sigma}{P_1P_4} + \frac{c_1(1-k)\sigma q P_5}{P_1P_4P_6}\right].$$

3.5. Local stability of the model (2.5)

It is highly imperative to investigate the local asymptotic stability of the new epidemiological model, which we accomplish by adopting Ulam-Hyers-Rassias (UHR) stability method in line with the work of Liu [40].

Definition 3.1. For $\Lambda(t) \in A^1([0,T],B)$, assume there exists $E_\upsilon > 0$ for $\upsilon > 0$. Then the proposed model (2.5) is generalized Ulam-Hyers-Rassias (UHR) Stable and for all solution

$$(S(t), E(t), Q(t), A(t), I(t), M(t), I_H(t), R(t)) \in A^1([0,T],B)$$

of the model (2.5), and is the existence of the following inequalities:

$$\begin{gathered}
|D_t^\varsigma S(t) - F(t,S(t))| \le \Lambda(t),\ |D_t^\varsigma E(t) - F(t,E(t))| \le \Lambda(t),\\
|D_t^\varsigma Q(t) - F(t,Q(t))| \le \Lambda(t),\\
|D_t^\varsigma A(t) - F(t,A(t))| \le \Lambda(t),\ |D_t^\varsigma I(t) - F(t,I(t))| \le \Lambda(t),\\
|D_t^\varsigma M(t) - F(t,M(t))| \le \Lambda(t),\\
|D_t^\varsigma I_H(t) - F(t,I_H(t))| \le \Lambda(t) \text{and } |D_t^\varsigma R(t) - F(t,R(t))| \le \Lambda(t).
\end{gathered}$$

The solution $(S(t), E(t), Q(t), A(t), I(t), M(t), I_H(t), R(t)) \in A^1([0,T],B)$ exists for the new model (2.5) with

$$\begin{gathered}
\left|S(t) - \bar{S}(t)\right| \le E_\upsilon\Lambda(t),\ \left|E(t) - \bar{E}(t)\right| \le E_\upsilon\Lambda(t),\ \left|Q(t) - \bar{Q}(t)\right| \le E_\upsilon\Lambda(t),\\
\left|A(t) - \bar{A}(t)\right| \le E_\upsilon\Lambda(t),\ \left|I(t) - \bar{I}(t)\right| \le E_\upsilon\Lambda(t),\ \left|M(t) - \bar{M}(t)\right| \le E_\upsilon\Lambda(t),\\
\left|I_H(t) - \bar{I}_H(t)\right| \le E_\upsilon\Lambda(t), \text{ and } \left|R(t) - \bar{R}(t)\right| \le E_\upsilon\Lambda(t).
\end{gathered}$$

Theorem 3.4. *With respect to $\Lambda(t) \in A^1([0,T],B)$, the fractional order model (2.5) is generalized Ulam-Hyers-Rassias (UHR) table given that*

$$(V_G, V_H, V_L, V_Q, V_R, V_S, V_T)\, T^\varsigma < 1.$$

Proof. Using definition 3.1, by denoting Λ as a non-decreasing function of t, then there exists $\upsilon > 0$, given that:

$$\int_0^t (t-\xi)^{\xi-1}\Lambda(t)\,d\zeta \le \upsilon\Lambda(t)$$

for every $t \in [0,T]$. Whereas, it has been demonstrated that the functions Q, T, U, V, W, X, Y, Z are continuous and $(J_Q, J_T, J_U, J_V, J_W, J_X, J_Y, J_Z) > 0$ satisfies the Lipchitz condition as it has been shown in the preceding section. From 3.2, the unique solution to fractional order model (2.5), is given by:

$$\bar{S}(t) = S(0) + \tfrac{1}{\Gamma(\xi)}\int_0^t (t-\zeta)^{\xi-1}F(t,S(t))d\zeta.$$

On integrating the inequalities in definition 3.1, we obtain:

$$\left|\bar{S}(t) - S(0) - \frac{1}{\Gamma(\xi)}\int_0^t (t-\zeta)^{\xi-1}F(t,S(t))d\zeta\right| \le \frac{1}{\Gamma(\xi)}\int_0^t (t-\zeta)^{\xi-1}\Delta(t)d\zeta$$

$$\leq \frac{\upsilon\Lambda(t)T^{\xi}}{\Gamma(\xi+1)}. \tag{3.12}$$

Using Lemma 2.1 and equation (3.12), yields

$$\begin{aligned}
&\left|S(t)-\bar{S}(t)\right| \\
\leq& S(t)-\left(S(0)+\frac{1}{\Gamma(\xi)}\int_0^t (t-\zeta)^{\varsigma-1}F(t,\bar{S}(t))d\zeta\right) \\
\leq& \Big|S(t)-S(0)-\Big(S(0)+\frac{1}{\Gamma(\varsigma)}\int_0^t (t-\zeta)^{\varsigma-1}F(t,\bar{S}(t))\,d\zeta \\
&+\frac{1}{\Gamma(\xi)}\int_0^t (t-\zeta)^{\xi-1}F(t,S(t))\,d\zeta-\frac{1}{\Gamma(\xi)}\int_0^t (t-\zeta)^{\xi-1}F(t,S(t))\,d\zeta\Big)\Big| \\
\leq& \Big|S(t)-S(0)+\frac{1}{\Gamma(\xi)}\int_0^t (t-\zeta)^{\xi-1}F(t,S(t))\,d\zeta\Big| \\
&+\frac{1}{\Gamma(\xi)}\int_0^t (t-\zeta)^{\xi-1}\left|F(t,S(t))-F(t,\bar{S}(t))\right|d\zeta \\
\leq& \frac{\upsilon\Lambda(t)T^{\xi}}{\Gamma(\xi+1)}+\frac{J_Q T^{\xi}}{\Gamma(\xi+1)}\int_0^t (t-\zeta)^{\xi-1}\left|F(t,S(t))-F(t,\bar{S}(t))\right|d\zeta \\
\Rightarrow& \left|S(t)-\bar{S}(t)\right| \leq \frac{\upsilon\Lambda(t)T^{\xi}}{\Gamma(\xi+1)}E_{\xi}\left(J_Q T^{\xi}\right).
\end{aligned}$$

By setting$E_{\xi}=\frac{\upsilon\Lambda(t)T^{\xi}}{\Gamma(\xi+1)}E_{\xi}\left(J_Q T^{\xi}\right)$, we obtain:

$$\left|S(t)-\bar{S}(t)\right| \leq E_{\xi}\Delta(t), t\in[0,T].$$

Similarly, by following the same approach, we obtain:

$$\begin{gathered}
\left|E(t)-\bar{E}(t)\right| \leq E_{\xi}\Lambda(t),\ \left|Q(t)-\bar{Q}(t)\right| \leq E_{\xi}\Lambda(t),\ \left|A(t)-\bar{A}(t)\right| \leq E_{\xi}\Lambda(t), \\
\left|I(t)-\bar{I}(t)\right| \leq E_{\xi}\Lambda(t),\ \left|M(t)-\bar{M}(t)\right| \leq E_{\xi}\Lambda(t),\ \left|I_H(t)-\bar{I}_H(t)\right| \leq E_{\xi}\Lambda(t) \\
\text{and } \left|R(t)-\bar{R}(t)\right| \leq E_{\xi}\Lambda(t),\ t\in[0,T].
\end{gathered}$$

From the foregoing, with regards to $\Lambda(t)$, generally, the indication is that the fractional order model (2.5) is Ulam-Hyers-Rassias (UHR) stable.

□

Theorem 3.4 demonstrates that the proposed fractional-order COVID-19 model (2.5) is generalized Ulam-Hyers-Rassias (UHR) stable under a specific condition on the model constants. Biologically, this means that small perturbations or uncertainties in the initial conditions, input data, or parameter values will not lead to large deviations in the model's solution. In the context of disease modeling, such stability ensures that the predicted disease dynamics (e.g., infection levels, recovery trends) remain robust and reliable, even if the data used for simulations are slightly imprecise due to measurement errors or incomplete reporting. This property is particularly important in real-world epidemiology, where data imperfections are common. Thus, UHR stability provides confidence in the model's use for forecasting and policy-making under uncertain conditions.

3.6. Global asymptotic stability of the fractional order model (2.5).

Theorem 3.5. *Whenever the reproduction number of the disease is greater than unity, $R_0 > 1$, the disease free equilibrium is globally asymptotically stable in domain D.*

Proof. We investigate the global asymptotic stability of the model (2.5) by using the method adopted by Castillo-Chavez [41].

$$D_t^{\xi} X = F(X, W) = \begin{bmatrix} -\frac{\beta_c(1-\rho_1)(1-\rho_2)(1-\tau_1)(c_1 A + I + c_2 M)S}{N} - vS + \mu Q \\ -\frac{\beta_c(1-\rho_1)(1-\rho_2)(1-\tau_1)(c_1 A + I + c_2 M)S}{N} - (\alpha + \sigma) E \\ \varepsilon_A A + \varepsilon_1 I + \varepsilon_M M + \gamma I_H - vS \\ \alpha E - (\eta + \mu) Q \end{bmatrix}. \tag{3.13}$$

$$F(X, 0) = \begin{bmatrix} -vS + \mu Q \\ -(\alpha + \sigma) E \\ \varepsilon_A A + \varepsilon_1 I + \varepsilon_M M + \gamma I_H - vS \\ \alpha E - (\eta + \mu) Q \end{bmatrix}. \tag{3.14}$$

$$\frac{dW}{dt} = \begin{vmatrix} k\sigma E - (\omega + \varepsilon_A) A \\ (1-k)\sigma E - (q + \delta_1 + \varepsilon_I) I \\ (1 - \tau_2 \varphi) qI - (\theta + \delta_M + \varepsilon_M) M \\ \eta Q + \omega A + \tau_2 \varphi q I + \theta M - (\gamma + \delta_H) I_H \end{vmatrix}. \tag{3.15}$$

$$A = \begin{vmatrix} -(\omega + \varepsilon_A) & 0 & 0 & 0 \\ 0 & -(q + \delta_I + \varepsilon_I) & 0 & 0 \\ 0 & (1 - \tau_2 \varphi) q & 0 & -(\theta + \delta_M + \varepsilon_M) \\ \omega & \tau_2 \varphi q & \theta & -(\gamma + \delta_H) \end{vmatrix}. \tag{3.16}$$

$$AW = \begin{vmatrix} \frac{A\beta(1-\rho_1)(1-\rho_2)(1-\tau_1)(S + k\sigma E - (\omega+\varepsilon_A)A)}{N} - A(\mu + k\sigma) \\ \frac{I\beta(1-\rho_1)(1-\rho_2)(1-\tau_1)(S + k\sigma E - (\omega+\varepsilon_A)A)}{N} - I(q + \delta_1 + \varepsilon_I) \\ \frac{M\beta(1-\rho_1)(1-\rho_2)(1-\tau_1)(S + k\sigma E - (\omega+\varepsilon_A)A)}{N} - M(\theta + \delta_M + \varepsilon_M) \\ A\omega + I\tau_2 \varphi q - (\gamma + \delta_H) M \end{vmatrix}. \tag{3.17}$$

$$\bar{G}(X, W) = AW - G(X, W) = \begin{bmatrix} A\omega \\ \tau_2 \varphi q I \\ 0 \end{bmatrix}.$$

Therefore, since $\bar{G}(X, W) \geq 0$, it shows that the disease free equilibrium of the proposed model (2.5) is globally asymptotically stable. □

Theorem 3.3 establishes that the disease-free equilibrium (DFE) of the proposed COVID-19 model is globally asymptotically stable in the feasible domain D whenever the basic reproduction number $R_0 > 1$. Biologically, this implies that when each infected individual generates more than one secondary case (i.e., the disease is spreading), the system does not return to the disease-free state regardless of initial population conditions. This means that the infection will persist in the population over time unless effective intervention strategies—such as mass vaccination, increased testing, social distancing, and public health education—are implemented to reduce R_0 below 1. This result underlines the importance of controlling transmission parameters to eliminate the disease and informs health policymakers that without sufficient control, the disease will remain endemic.

3.7. Numerical scheme and algorithm

Given that $t_j = jh$ for $j = 0, 1, 2, ...n$, is a uniformed grid point represented by some integer n for the step size given by $h = {}^{M}/_{v}$. By using the piece-wise interpolation, knots and nodes located at t_k for $k = 0, 1, 2, ...j + 1$, the one-step Adam-Moulton's method for fractional order version reduces to corrector formula as described in Diethelm et al. [43] given by equation (3.18) below:

$$
\begin{aligned}
S(t_{j+1}) - S(0) &= \frac{h^{\xi}}{\Gamma(\xi+2)}\left(\sum_{k=0}^{j}\eta_{k,j+1}Q(t_k, S(t_k)) + Q(t_{j+1}, S^q(t_{j+1}))\right),\\
E(t_{j+1}) - E(0) &= \frac{h^{\xi}}{\Gamma(\xi+2)}\left(\sum_{k=0}^{j}\eta_{k,j+1}T(t_k, S(t_k)) + T(t_{j+1}, E^q(t_{j+1}))\right),\\
Q(t_{j+1}) - Q(0) &= \frac{h^{\xi}}{\Gamma(\xi+2)}\left(\sum_{k=0}^{j}\eta_{k,j+1}U(t_k, S(t_k)) + U(t_{j+1}, Q^q(t_{j+1}))\right),\\
A(t_{j+1}) - A(0) &= \frac{h^{\xi}}{\Gamma(\xi+2)}\left(\sum_{k=0}^{j}\eta_{k,j+1}V(t_k, S(t_k)) + V(t_{j+1}, A^q(t_{j+1}))\right),\\
I(t_{j+1}) - I(0) &= \frac{h^{\xi}}{\Gamma(\xi+2)}\left(\sum_{k=0}^{j}\eta_{k,j+1}W(t_k, S(t_k)) + W(t_{j+1}, I^q(t_{j+1}))\right),\\
M(t_{q+1}) - M(0) &= \frac{h^{\varsigma}}{\Gamma(\varsigma+2)}\left(\sum_{i=0}^{q}\eta_{i,q+1}X(t_i, I_{cp}(t_i)) + X(t_{q+1}, M^y(t_{q+1}))\right),\\
I_H(t_{q+1}) - I_H(0) &= \frac{h^{\varsigma}}{\Gamma(\varsigma+2)}\left(\sum_{i=0}^{q}\eta_{i,q+1}Y(t_i, I_{cp}(t_i)) + Y\left(t_{q+1}, I_{cp}^y(t_{q+1})\right)\right),\\
R(t_{q+1}) - R(0) &= \frac{h^{\varsigma}}{\Gamma(\varsigma+2)}\left(\sum_{i=0}^{q}\eta_{i,q+1}Z(t_i, I_{cp}(t_i)) + Z(t_{q+1}, R^y(t_{q+1}))\right),
\end{aligned}
\tag{3.18}
$$

with the weight:

$$\eta_{k,j+1} = \begin{cases} j^{\xi+1} - (j-\xi)(j+1)^{\xi}, & k = 0, \\ (j-k+2)^{\xi+1} + (j-1)^{\xi+1} - 2(j-k+1)^{\xi+1}, & 1 \le k \le j, \\ 1, & k = j+1. \end{cases}$$

The predictor formula which is based on the famous one-step Adams-Bashforth method is given by:

$$\begin{aligned} S^q(t_{j+1}) - S(0) &= \frac{1}{\Gamma(\xi)} \sum_{k=0}^{j} \upsilon_{k,j+1} Q(t_k, S(t_k)), \\ E^q(t_{j+1}) - E(0) &= \frac{1}{\Gamma(\xi)} \sum_{k=0}^{j} \upsilon_{k,j+1} T(t_k, E(t_k)), \\ Q^q(t_{j+1}) - Q(0) &= \frac{1}{\Gamma(\xi)} \sum_{k=0}^{j} \upsilon_{k,j+1} U(t_k, Q(t_k)), \\ A^q(t_{j+1}) - A(0) &= \frac{1}{\Gamma(\xi)} \sum_{k=0}^{j} \upsilon_{k,j+1} V(t_k, A(t_k)), \\ I^q(t_{j+1}) - I(0) &= \frac{1}{\Gamma(\xi)} \sum_{k=0}^{j} \upsilon_{k,j+1} W(t_k, I(t_k)), \\ M^q(t_{j+1}) - M(0) &= \frac{1}{\Gamma(\xi)} \sum_{k=0}^{j} \upsilon_{k,j+1} X(t_k, M(t_k)), \\ I_H^y(t_{j+1}) - I_H(0) &= \frac{1}{\Gamma(\xi)} \sum_{k=0}^{j} \upsilon_{k,j+1} Y(t_k, I_H(t_k)), \\ R^q(t_{j+1}) - R(0) &= \frac{1}{\Gamma(\xi)} \sum_{k=0}^{j} \upsilon_{k,j+1} Z(t_k, I(t_k)), \end{aligned} \tag{3.19}$$

together with weight:

$$\upsilon_{k,j+1} = \xi^{-1} h^{\xi} (j-k+1)^{\xi} - (j-k)^{\xi}.$$

3.8. Numerical simulations

In this study, we adopt the nonstandard finite difference (NSFD) scheme to numerically approximate the solution of the Caputo-based fractional-order COVID-19 model. The choice of the NSFD scheme is motivated by its ability to preserve essential qualitative features of the original continuous model, including the positivity and boundedness of the state variables, which are crucial in modeling epidemiological dynamics. Traditional numerical methods such as Euler or Runge-Kutta schemes may fail to retain these biological properties, especially when dealing with nonlinear fractional-order systems. The NSFD scheme, through its non-local discretization and flexible denominator functions, ensures numerical stability, convergence, and adherence to the inherent memory effect of the fractional derivative. This makes

it a more robust and accurate method for simulating the long-term behavior of infectious disease models, particularly those involving memory-dependent processes like COVID-19. From qualitative analysis of the new model (2.5), some vital results were obtained. It becomes highly imperative to validate these results; consequently, there is the need to do numerical simulation of the model. In addition, numerical simulation of the model is a necessity in the sense that it is the basis for generating empirical-based epidemiological findings that will assist policy makers in the health sector to procure measures that will help in combatting the scourge of the disease. We employ the predictor-corrector method derived from Adams-Bashforth linear multistep method which is based on the famous Caputo fractional order derivatives.

4. Data fitting to model for estimation of parameter values

We performed the data fitting to our model by using the fmincon algorithm contained in the optimization tool box of MATLAB computation programming software. The procedure of using this routine is by minimization of the squared differences between observed cumulative active cases data point and the corresponding case point as obtained from our model (2.5). Our data fitting to model was implemented for epidemic period in Nigeria from 9th July 2021 to 17th September 2021 by using the daily cumulative number of active-cases of the disease as obtained from Nigeria authority, NCDC. In the spirits of the work of Okunoghae and Omame [18] that modelled the dynamics of the COVID-19 pandemic in Lagos Nigeria, some of our parameters were estimated as $\sigma = 0.015$ per day, $\alpha = {}^{1}/_{7}$ per day, $\delta_1 = \delta_M = 0.015$ and $\delta_H = 0.21$ per day, $\gamma = {}^{1}/_{15}$ per day. In addition, other parameters such as β_c, θ, q, η and ω were estimated via fitting the model (2.5) with the daily number of active cases and cumulative number of reported cases. On the other hand, $E(0)$, $E_Q(0)$and $I_H(0)$; the numbers of those individuals latently infected, those quarantined and infectious individuals that were detected and hospitalized on the 1st of December 2021 will be estimated from the data fitting. We noted that the population of Nigeria is 206,603,134 consequently. We took this number as the starting point, that is, the initial condition for our simulation, hence we set S(0)= 206,603,134, $E(0) = 200000$, $Q(0) = 7000$,$A(0) = 30000$, $I(0) = 150000$, $M(0) = 50000$, while we set $I_H(0) = 1719$ and $R(0) = 164415$. It should be noted that this is done considering the date of index case. It is pertinent to note that we performed the model fitting by using the fmincon algorithm in MATLAB and we implemented the model fitting for a period of new wave of the epidemic from 9th July to 17th September, 2021 when the sub-Saharan country of Nigeria came heavily affected by the deadly disease.

In the table below is the real life data pertaining to the deadly disease obtained from Nigerian authority, Nigeria Centre for Disease Control (NCDC) for the period when the third wave of the pandemic pervaded the air in Nigeria from 9th July 2021 to 17th September 2021.

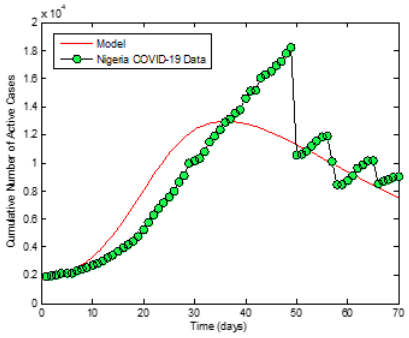

Figure 2. Model fitting

Date	July 9	July 10	July 11	July 12	July 13	July 14	July 15	July 16	July 17
Case	1897	1987	1989	2113	2119	2138	2286	2414	2531

Date	July 18	July 19	July 20	July 21	July 22	July 23	July 24	July 25	July 26
Case	2706	2840	3023	3251	3404	3712	3975	4190	4392

Date	July 27	July 28	July 29	July 30	July 31	Aug 1	Aug 2	Aug 3	Aug 4
Case	4757	5238	5750	6284	6765	7161	7562	7979	8636

Date	Aug 5	Aug 6	Aug 7	Aug 8	Aug 9	Aug 10	Aug 12	Aug 13	Aug 14
Case	9076	9090	10003	10136	10334	10793	11510	11901	12377

Date	Aug 15	Aug 16	Aug 17	Aug 18	Aug 19	Aug 20	Aug 21	Aug 22	Aug 23
Case	12917	13152	13554	13756	14619	15100	15200	16055	16300

Date	Aug 24	Aug 25	Aug 26	Aug 27	Aug 28	Aug 29	Aug 30	Aug 31	Sep 1
Case	16927	17210	17791	18210	10575	10608	10858	10608	10858

Date	Sep 2	Sep 3	Sep 4	Sep 5	Sep 6	Sep 7	Sep 8	Sep 9	Sep 10
Case	11203	11533	11862	11914	10067	8430	8452	8755	9089

Date	Sep 11	Sep 12	Sep 13	Sep 14	Sep 15	Sep 16	Sep 17
Case	9591	9871	10121	10135	8492	8701	8799

Table 3. Cumulative active COVID-19 cases for Nigeria from July 9, 2021 to September 17, 2021. Source: [19].

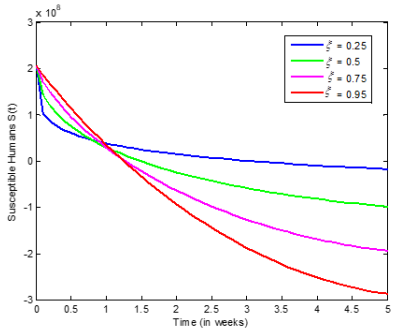

Figure 3. The plot of the approximate solution of susceptible humans with different fractional values of ξ

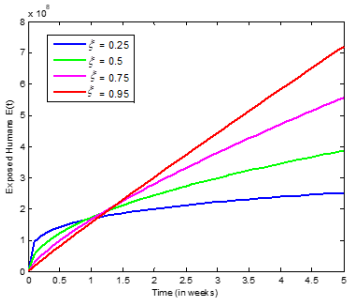

Figure 4. The plot of the approximate solution of exposed humans with different fractional values of ξ

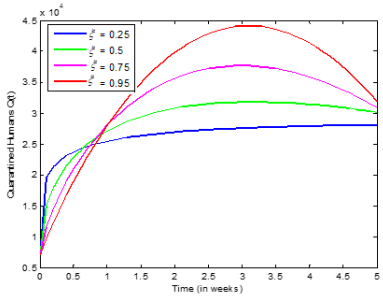

Figure 5. The plot of the approximate solution of quarantined humans with different fractional values of ξ

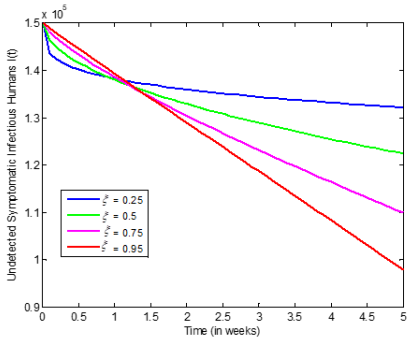

Figure 6. The plot of the approximate solution of the undetected symptomatic infectious humans with different fractional values of ξ

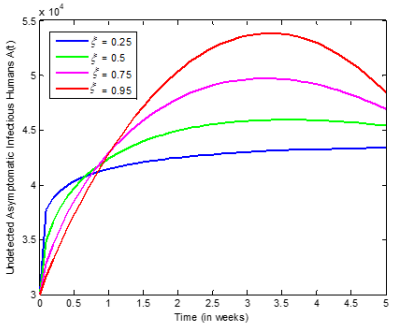

Figure 7. The plot of the approximate solution of the undetected asymptomatic infectious humans with different fractional values of ξ

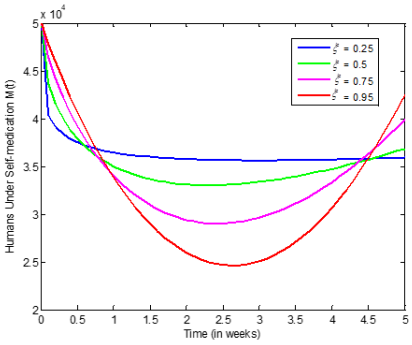

Figure 8. The plot of the approximate solution of the humans under self-medication with different fractional values of ξ

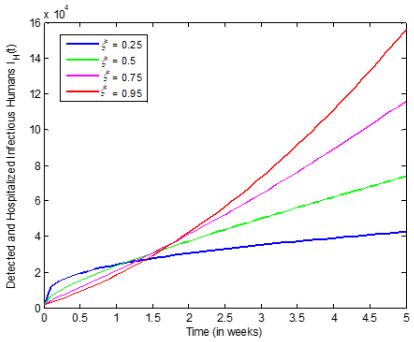

Figure 9. The plot of the approximate solution of the detected and hospitalized humans with different fractional values of ξ

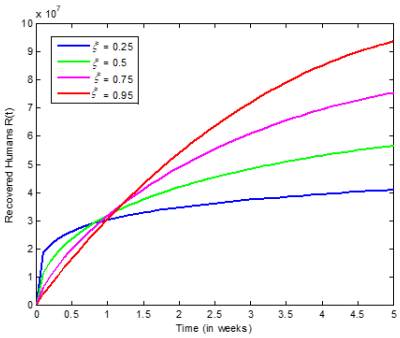

Figure 10. The plot of the approximate solution the recovered class with different fractional values of ξ

We present results for simulation of the model over a period of 5 weeks using different fractional orders $\xi = 0.25,\ 0.5,\ 0.75,\ 0.98$. From Figure 3, observe that as the fractional order of the fractional derivative ξ increases the number of individuals that are susceptible to the disease decreases proportionately. It shows that this is a good result in the control of the disease. From Figure 4, it could be seen that as the order of the fractional derivative ξ is increasing, it leads to proportional decrease in the number of the individuals exposed to the deadly disease. Figure 5 and Figure 6 show the same results as that in Figure 4. In Figure 7, looking at each of the curves on the figure, observe that there is a downward trend meaning that number of undetected asymptomatic individuals decreases over time as from the first day of the third wave of the pandemic. By considering the curves on the figure as a whole, observe that as the fractional order ξ increases, it leads to a proportional increase in undetected asymptomatic individuals over time.

In Figure 8, the number of individuals under self-medication for each of the curves on the figure starts decreasing in value from the first day when the third wave of the disease started in Nigeria till about the fifth day to two and half weeks before their values start going up again. From Figure 9, it can be seen that for all the curves, the number of detected and hospitalized infectious individuals is in the upward trend, meaning that their number starts going up as from the first day that the third wave of COVID-19 pandemic started for each of the fractional order ξ.

Generally, it can be seen from Figure 9 that as the fractional order ξ increases, the number of detected and hospitalized infectious individuals keeps increasing too.

From Figure 10, each of the curves is on the upward trend, meaning that the number of recovered individuals increases over time. And generally, as the fractional order ξ increases, it leads to a proportional increase in the number of recovered individuals. The observed variation in the size of infected compartments under different fractional orders can be attributed to the nature of the Caputo fractional operator with singular kernel used in this study. This operator incorporates memory effects through its non-local integral structure, allowing the model to consider the historical states of the system in determining the present dynamics. This characteristic introduces a smoothing and stabilizing influence on the infection spread, especially under long-term interventions. Notably, the results show that as the fractional order ξ decreases, indicating stronger memory, the infected populations are reduced accordingly. This demonstrates that the Caputo operator enhances the stability of infected compartments by tempering abrupt changes and allowing gradual transitions, which aligns better with real-world disease behavior. Therefore, the memory effect inherent in the fractional operator plays a crucial role in capturing the prolonged impact of prior exposures and interventions on current disease dynamics.

5. Conclusion

Motivated by the merits of fractional order models consisting systems of fractional order differential equations over the classical order integer models which are of non-linear differential equations in classical order integer, we extended the work of Omede et al. [10] by reformulating their classical order integer model as fractional order model. By adopting Laplace transform, we showed that the state variables of the model are positive at all times and showed the existence and uniqueness of solution for the model by Schaefer's fixed point theorem. We went further in analysis of the model and showed that the model is Ulam-Hyers-Rassias stable and that its disease-free equilibrium is locally and globally asymptotically stable whenever the reproduction number of the disease is less than unity. The implication of this is that the disease will be brought under control when measures are taken to keep the reproduction of the disease at a value less than unity. The novelty of our work is that we did the parameters estimates for the fractional order model by fitting our model to real-life data obtained about the disease under study, COVID-19 other than obtaining all of them from the literature and just making assumptions where they could not be so obtained. The revelation from the numerical simulation of the fractional order model is that it gives more degrees of freedom as the order of the fractional differential equations contained in the model can be varied with ease in order to show responses by different classes in real time. Furthermore, it was observed that as there is a reduction in the order of the fractional derivative, it is accompanied with reduction in the value of the population of each of the infected classes in the model. From the analysis and numerical simulations presented in this study we conclude that the fractional-order COVID-19 model using Caputo derivatives effectively captures the memory effects of disease transmission and progression, which are not accounted for in classical models. Also, the variation of the fractional order ξ reveals that system dynamics are highly sensitive to changes in ξ, offering a flexible tool for studying a wide range of possible epidemic scenarios. Similarly, the proof of Ulam-Hyers-Rassias stability confirms the model's robustness under

small perturbations, while the local and global stability of the disease-free equilibrium ensures theoretical reliability under realistic conditions. Finally, fitting the model to real epidemiological data from Nigeria validates the model's practical relevance and demonstrates the potential of fractional-order models to support public health decision-making, especially in settings with complex transmission patterns. The results from numerical simulations reveal that the fractional-order model offers greater flexibility than classical models. Specifically, the fractional order ξ allows for dynamic adjustment of system behavior, which captures real-time responses in different compartments. It was observed that decreasing the order ξ leads to a corresponding reduction in the population of infected individuals, highlighting the memory-dependent nature of disease transmission dynamics. From both the theoretical analysis and numerical simulations, we conclude that the fractional-order COVID-19 model formulated with Caputo derivatives effectively accounts for memory effects in disease transmission and progression, which are absent in classical integer-order models. Furthermore, the system's sensitivity to changes in ξ offers a powerful tool for simulating a wide range of epidemic scenarios. The proven Ulam-Hyers-Rassias stability guarantees robustness of the model under small perturbations, while the established stability of the disease-free equilibrium validates the model's theoretical soundness. It is pertinent to note that the fractional-order model formulated in this work does not incorporate further disease control strategies such as optimal control, which could be explored in future studies. Beyond this, several potential extensions exist. For instance, alternative fractional operators like the Atangana-Baleanu or Caputo-Fabrizio derivatives may be employed to investigate the influence of different memory kernels on disease dynamics. The model can also be enhanced by incorporating spatial heterogeneity, age-structured populations, or stochastic elements to reflect more realistic transmission settings. Additionally, integrating machine learning or real-time data assimilation techniques could significantly improve the model's forecasting and policy-evaluation capabilities. These directions represent promising avenues to further strengthen the relevance and applicability of fractional-order epidemic models.

References

[1] J. A. Kucharski, T. W. Russell, C. Diamond, Y. Liu, J. Edmunds, S. Funk, M. E. Rosalind, *Early dynamics of transmission and control of COVID-19: A mathematical modelling study*, Lancet Infect. Dis. **20** (2020) 553–568.

[2] I. Aslan, M. Demir, M. G. Wise, S. Lenhart, *Modeling COVID-19: forecasting and analyzing the dynamics of the outbreak in Hubei and Turkey*, (2020).

[3] A. Atangana, *Modelling the spread of COVID-19 with new fractal-fractional operators: can the lockdown save mankind before vaccination*, Chaos Solitons Fractals, (2020).

[4] Y. Bai, L. Yao, T. Wei, F. Tian, D.Y. Jin, L. Chen, M. Wang, *Presumed asymptomatic carrier transmission of COVID-19*, JAMA (2020).

[5] A. Enahoro, O. Iboi, O. Sharomi, C. N. Ngonghala, A. B. Gumel, *Mathematical modeling and analysis of covid-19 pandemic in Nigeria*, Mathematical Biosciences and Engineering, **17** (6) (2020) 7192–7220.

[6] F. P. Polack, S. J. Thomas, N. Kitchin, J. Absalon, A. Gurtman, S. Lockhart, J. L. Perez, G. Pérez Marc, E. Moreira, C. Zerbini, R. Bailey, K. A. Swanson,

S. Roychoudhury, K. Koury, P. Li, W. V. Kalina, D. Cooper, R. W. Frenck Jr., S. Hammitt, Ö. Türeci, U. Nelluri, S. Tresnan, S. Mather, P. R. Dormitzer, U. Şahin, K. U. Jansen, W. C. Gruber, *Safety and Efficacy of the BNT162b2 mRNA Covid-19 Vaccine*, N. Engl. J. Med., (2020).

[7] R. Patel, M. Kaki, V. S. Potluri, P. Kahar, D. Khanna, *A comprehensive review of SARS-CoV-2 vaccines: Pfizer, Moderna & Johnson & Johnson*, Hum. Vaccin. Immunother., (2022).

[8] S. M. Blower, H. Dowlatabadi, *Sensitivity and uncertainty analysis of complex models of disease transmission: an HIV model, as an example*, International Statistical Review/Revenue Internationale de Statistique, (1994) 229–243.

[9] B. I. Omede, P. O. Ameh, A. Omame, A. Abdullahi, Bolarinwa Bolaji, *Modelling the transmission dynamics of Nipah virus with optimal control*, J. Math. Comput. Sci. **11** (2021) 5813–5846.

[10] B. I. Omede, U. B. Odionyenma, A. A. Ibrahim, Bolarinwa Bolaji, *Third wave of COVID-19: mathematical model with optimal control strategy for reducing the disease burden in Nigeria*, Int. J. Dynam. Control, (2022).

[11] A. K. Muhammad, A. Atangana, *Modeling the dynamics of novel coronavirus (2019-nCov) with fractional derivative*, Alexandria Engineering Journal, (2020).

[12] K. Shah, H. Khalil, R. A. Khan, *Analytical solutions of fractional order diffusion equations by natural transform method*, Iranian Journal of Science and Technology **14** (2016).

[13] N. M. Ferguson, D. Laydon, G. Nedjati-Gilani, N. Imai, K. Ainslie, M. Baguelin, S. Bhatia, A. Boonyasiri, Z. Cucunubá, G. Cuomo-Dannenburg, *Impact of non-pharmaceutical interventions (NPIs) to reduce COVID-19 mortality and healthcare demand*, vol. 16 Imperial College COVID-19 Response Team, London, (2020).

[14] B. Ivorra, M. R. Ferrandez, M. Vela-Perez, A. M. Ramos, *Mathematical modelling of the spread of the coronavirus disease 2019 (COVID-19) taking into account the undetected infections. The case of China*, Commun. Nonlinear Sci. Numer. Simulat. (2020).

[15] M. A. Khan, A. Atangana, *Modeling the dynamics of novel coronavirus 2019-nCoV with fractional derivative*, Alexandria Eng. J. (2020).

[16] A. G. Gumel, E. A. Iboi, C. N. Ngonghala, E. H. Elbasha, *A primer on using Mathematics to understand COVID-19 dynamics: Modeling, analysis and simulations*, Infectious Disease Modelling **6** (2021) 148–168.

[17] A. I. Abioye, O. J. Peter, H. A. Ogunseye, F. A. Oguntolu, K. Oshinubi, A. A. Ibrahim, I. Khan, *Mathematical Model of COVID-19 in Nigeria with Optimal Control*, Results in Physics, (2021).

[18] D. Okuonghae, A. Omame, *Analysis of a mathematical model for COVID-19 population dynamics in Lagos, Nigeria*, Chaos, Solitons and Fractals **139** (2020).

[19] Nigeria Centre for Disease Control and Prevention, *An update of COVID-19 outbreak in Nigeria*, https://ncdc.gov.ng/diseases/sitreps/?cat=14&name=AnupdateofCOVID-19outbreakinNigeria, (2021).

[20] A. Omame, M. Abbas, C. P. Onyenegecha, *A fractional order model for the co-interaction of COVID-19 and Hepatitis B virus*, Results in Physics (2022).

[21] E. Shim, A. Tariq, W. Choi, Y. Lee, G. Chowell, *Transmission potential and severity of COVID-19 in South Korea*, Int. J. Infect. Dis. (2020).

[22] C. Tian-Mu, Jia Rui, W. Qiu-Peng, Ze-Yu Zhao, Jing-An Cui, Ling Yin, *A Mathematical model for simulating the phase-based transmissibility of a novel coronavirus*, Infectious Diseases of Poverty (2020).

[23] L. Xue, S. Jing, J. C. Miller, W. Sun, H. Li, J. G. Estrada-Franco, M. Hyman, H. Zhu, *data-driven network model for the emerging COVID-19 epidemics in Wuhan, Toronto and Italy*, Math. Biosci. (2020) 1–20.

[24] A. Yousefpour, H. Jahanshahi, S. Bekiros, *Optimal policies for control of the novel coronavirus disease (COVID-19) outbreak*, Chaos Solitons Fractals **136** (2020) 109883.

[25] S. O. Sowole, A. A. Ibrahim, D. Sangare, I. O. Ibrahim, F. I. Johnson, *Understanding the Early Evolution of COVID-19 Disease Spread Using Mathematical Model and Machine Learning Approaches*, Global Journal of Science Frontier Research, (2020) 19–36.

[26] M. A. Shereen, S. Khan, A. Kazmi, N. Bashir, R. Siddique, *COVID-19 infection: Origin, transmission, and characteristics of human coronaviruses*, Journal of Advanced Research, (2020).

[27] A. Atangana, A. Secer, *A Note on Fractional Order Derivatives and Table of Fractional Derivatives of Some Special Functions*, Abstract Applied Analysis, Article ID 279681, (2013).

[28] S. G. Samko, A. A. Kilbas, O. I. Maritchev, *Integrals and Derivatives of the Fractional Order and Some of Their Applications*, in Russian, Nauka i Tekhnika, Minsk, Belarus, (1987).

[29] I. Podlubny, *Geometric and physical interpretation of fractional integration and fractional differentiation*, Fractional Calculus and Applied Analysis **5**(4) (2002) 367–386.

[30] M. Caputo, *Linear models of dissipation whose Q is almost frequency independent*, Annals of Geophysics **19**(4) (1966) 383–393.

[31] A. Atangana, *Numerical solution of space-time fractional derivative of groundwater flow equation*, in Proceedings of the International Conference of Algebra and Applied Analysis, Istanbul, Turkey, (2012) 20.

[32] G. Jumarie, *On the solution of the stochastic differential equation of exponential growth driven by fractional Brownian motion*, Applied Mathematics Letters **18**(7) (2005) 817–826.

[33] G. Jumarie, *Modified Riemann-Liouville derivative and fractional Taylor series of non-differentiable functions further results*, Computers & Mathematics with Applications **51** (2006) 1367–1376.

[34] C. F. M. Coimbra, *Mechanics with variable-order differential operators*, Annalen der Physik **12** (2003) 692–703.

[35] M. Caputo, M. Fabrizio, *A new definition of fractional derivative without singular kernel*, Progress in Fractional Differentiation and Applications **1**(2) (2015) 1–3.

[36] A. Atangana, D. Baleanu, *New fractional derivatives with nonlocal and non-singular kernel: theory and applications to heat transfer model*, Therm. Sci. **20**(2) (2016) 763–769.

[37] K. Ugochukwu Nwajeri, Andrew Omame, Chibueze Onyenegecha, *Analysis of a fractional order model for HPV and CT co-infection*, Results in Physics **28** (2021) 104643.

[38] S. Ndolane, *SIR epidemic model with Mittag-Lefler fractional derivative*, Chaos Solitons Fractals **137** (2020) 109833.

[39] P. van den Driessche, J. Watmough, *Reproduction numbers and sub-threshold endemic equilibria for compartmental models of disease transmission*, Math. Biosci. **180** (2002) 29–48.

[40] K. Liu, M. Feckan, J. Wang, *Hyers-Ulam stability and existence of solutions to the generalized Liouville-Caputo fractional differential equations*, Symmetry **12**(6) (2020) 955.

[41] C. Castillo-Chavez, Z. Feng, W. Huang, *On the computation of R_0 and its role on global stability*, In Mathematical Approaches for Emerging and Re-emerging Infectious Diseases: An Introduction **125** (2002) 229–250.

[42] K. Diethelm, A. D. Freed, *The FracPECE subroutine for the numerical solution of differential equations of fractional order*, Forschung und Wissenschaftliches Rechnen, (1998) 57–71.

[43] C. Xu, D. Mu, Z. Liu, Y. Pang, M. Liao, C. Aouiti, *New insight into bifurcation of fractional-order 4D neural networks incorporating two different time delays*, Communications in Nonlinear Science and Numerical Simulation **118** (2023) 107043.

[44] C. Xu, Z. Liu, P. Li, J. Yan, L. Yao, *Bifurcation mechanism for fractional-order three triangle multi-delayed neural networks*, Neural Processing Letters, (2022).

[45] C. Xu, W. Zhang, C. Aouiti, Z. Liu, L. Yao, *Bifurcation insight for a fractional-order stage structure predator-prey system incorporating mixed time delays*, Mathematical Methods in the Applied Sciences, (2023).

[46] A. Omame, D. Okuonghae, U. K. Nwajeri, C. P. Onyenegecha, *A fractional-order multi vaccination model for COVID-19 with non-singular kernel*, Alexandria Engineering Journal **61**(8) (2022) 6089–6104.

[47] A. Omame, U. K. Nwajeri, M. Abbas, C. P. Onyenegecha, *A fractional order control model for Diabetes and COVID-19 co-dynamics with Mittag-Leffler function*, Alexandria Engineering Journal **61**(10) (2022) 7619–7635.

[48] X. He, E. H. Y. Lau, P. Peng, X. Deng, J. Wang, X. Hao, Y. C. Lau, J. Y. Wong, Y. Guan, X. Tan, X. Mo, Y. Chen, B. Jiao, W. Chen, F. He, T. Zhang, A. Lo, L.-M. Ho, X. Song, W. Leung, M. M. H. Sy, R. Valkenburg, O. T. Y. Tsang, S.-Y. Chan, J. S. M. Peiris, G. M. Leung, B. J. Cowling, *Temporal dynamics in viral shedding and transmissibility of COVID-19*, Nature Medicine **26**(5) (2020) 672–675.

[49] D. P. Oran, E. J. Topol, *Prevalence of asymptomatic SARS-CoV-2 infection*, Annals of Internal Medicine **173**(5) (2020) 362–367.

[50] M. Gandhi, D. S. Yokoe, D. V. Havlir, *Asymptomatic transmission, the Achilles' heel of current strategies to control Covid-19*, New England Journal of Medicine **382**(22) (2020) 2158–2160.

[51] Q. Bi, Y. Wu, S. Mei, C. Ye, X. Zou, Z. Zhang, X. Liu, L. Wei, S. A. Truelove, T. Zhang, W. Gao, C. Cheng, X. Tang, X. Wu, Y. Wu, B. Sun, S. Huang, Y. Sun, J. Zhang, T. Ma, J. Lessler, T. Feng, *Epidemiology and transmission of COVID-19 in 391 cases and 1286 of their close contacts in Shenzhen, China: a retrospective cohort study*, The Lancet Infectious Diseases **20**(8) (2020) 911–919.

[52] D. K. Chu, E. A. Akl, S. Duda, K. Solo, S. Yaacoub, H. J. Schünemann, COVID-19 Systematic Urgent Review Group Effort (SURGE) study authors, *Physical distancing, face masks, and eye protection to prevent person-to-person transmission of SARS-CoV-2 and COVID-19: a systematic review and meta-analysis*, The Lancet **395**(10242) (2020) 1973–1987.

[53] A. El-Mesady, O. J. Peter, A. Omame, F. A. Oguntolu, *Mathematical analysis of a novel fractional order vaccination model for Tuberculosis incorporating susceptible class with underlying ailment*, International Journal of Modelling and Simulation, (2024) 1–25.

[54] O. J. Peter, N. D. Fahrani, Fatmawati, Windarto, C. W. Chukwu, *A fractional derivative modeling study for measles infection with double dose vaccination*, Healthcare Analytics **4** (2023) 100231.

[55] E. Addai, A. Adeniji, O. J. Peter, J. O. Agbaje, K. Oshinubi, *Dynamics of age-structure smoking models with government intervention coverage under fractal-fractional order derivatives*, Fractal and Fractional **7**(5) (2023) 370.

[56] P. Yadav, S. Jahan, K. Shah, O. J. Peter, T. Abdeljawad, *Fractional-order modelling and analysis of diabetes mellitus: Utilizing the Atangana-Baleanu Caputo (ABC) operator*, Alexandria Engineering Journal **81** (2023) 200–209.

[57] A. I. Abioye, O. J. Peter, H. A. Ogunseye, F. A. Oguntolu, T. A. Ayoola, A. O. Oladapo, *A fractional-order mathematical model for malaria and COVID-19 co-infection dynamics*, Healthcare Analytics **4** (2023) 100210.

[58] O. J. Peter, A. Yusuf, M. M. Ojo et al., *A mathematical model analysis of meningitis with treatment and vaccination in fractional derivatives*, International Journal of Applied and Computational Mathematics **8** (2022) 117.

[59] O. J. Peter, F. A. Oguntolu, M. M. Ojo, A. O. Oyeniyi, R. Jan, I. Khan, *Fractional order mathematical model of monkeypox transmission dynamics*, Physica Scripta **97**(8) (2022) 084005.

[60] A. I. Abioye, O. J. Peter, H. A. Ogunseye, F. A. Oguntolu, K. Oshinubi, A. A. Ibrahim, I. Khan, *Analysis and dynamics of fractional order mathematical model of COVID-19 in Nigeria using Atangana-Baleanu operator*, Computers, Materials & Continua **66**(2) (2021) 1823–1848.

[61] O. J. Peter, F. A. Oguntolu, M. M. Ojo, A. O. Oyeniyi, R. Jan, I. Khan, *Fractional order of pneumococcal pneumonia infection model with Caputo Fabrizio operator*, Results in Physics **29** (2021) 104581.

[62] M. M. Ojo, O. J. Peter, E. F. D. Goufo, H. S. Panigoro, F. A. Oguntolu, *Transmission dynamics of fractional order brucellosis model using Caputo-Fabrizio operator*, International Journal of Differential Equations **2020** (2020) 2791380.